

UCSF

UC San Francisco Previously Published Works

Title

CD4+ Group 1 Innate Lymphoid Cells (ILC) Form a Functionally Distinct ILC Subset That Is Increased in Systemic Sclerosis

Permalink

<https://escholarship.org/uc/item/17f49320>

Journal

The Journal of Immunology, 196(5)

ISSN

0022-1767

Authors

Roan, Florence
Stoklasek, Thomas A
Whalen, Elizabeth
[et al.](#)

Publication Date

2016-03-01

DOI

10.4049/jimmunol.1501491

Peer reviewed

Publication Charges and Reprints

There has been a change in our author billing and reprint ordering system. Publication charges and reprint orders are now handled by Dartmouth Journal Services using a web-based system.

Within the next 24 hours you will receive an e-mail from aubilling.djs@sheridan.com. This e-mail will include a link to an online reprint order form and to an estimate of your publication charges. From this secure website you will be able to review the estimated charges for your article and order reprints. Please log in to this website as soon as possible to ensure that there will be no delay to your article being published.

Please note that this is a change in procedure. If you have questions regarding this change, about the e-mail you will receive, or about the website, please contact aubilling.djs@sheridan.com or call 802-560-8518.

Annotating PDFs using Adobe Reader XI

Version 1.4 January 14, 2014

1. Update to Adobe Reader XI

The screen images in this document were captured on a Windows PC running Adobe Reader XI. Editing of DJS proofs requires the use of Acrobat or Reader XI or higher. At the time of this writing, Adobe Reader XI is freely available and can be downloaded from <http://get.adobe.com/reader/>

2. What are eProofs?

eProof files are self-contained PDF documents for viewing on-screen and for printing. They contain all appropriate formatting and fonts to ensure correct rendering on-screen and when printing hardcopy. DJS sends eProofs that can be viewed, annotated, and printed using the free version of Acrobat Reader XI (or higher).

3. Comment & Markup toolbar functionality

A. Show the Comment & Markup toolbar

The Comment & Markup toolbar doesn't appear by default. Do one of the following:

- Select View > Comment > Annotations.
- Click the Comment button in the Task toolbar.

Note: If you've tried these steps and the Annotation Tools do not appear, make sure you have updated to version XI or higher.

B. Select a commenting or markup tool from the Annotations window.

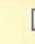

Note: After an initial comment is made, the tool changes back to the Select tool so that the comment can be moved, resized, or edited. (The Pencil, Highlight Text, and Line tools stay selected.)

C. Keep a commenting tool selected

Multiple comments can be added without reselecting the tool. Select the tool to use (but don't use it yet).

- Right Click on the tool.
- Select Keep Tool Selected.

4. Using the comment and markup tools

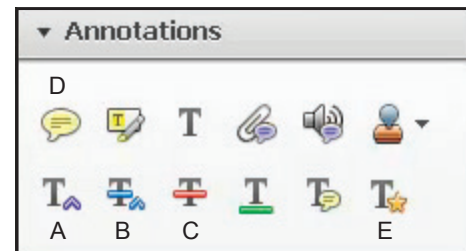
To *insert*, *delete*, or *replace* text, use the corresponding tool. Select the tool, then select the text with the cursor (or simply position it) and begin typing. A pop-up note will appear based upon the modification (e.g., inserted text, replacement text, etc.). Use the Properties bar to format text in pop-up notes. A pop-up note can be minimized by selecting the  button inside it. A color-coded  symbol will remain behind to indicate where your comment was inserted, and the comment will be visible in the Comments List.

5. The Properties bar

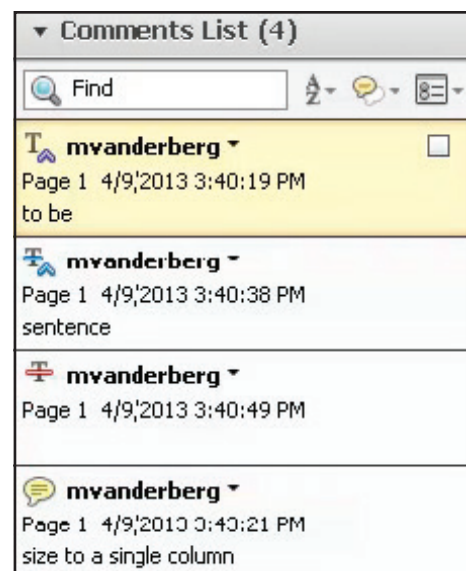
The Properties bar can be used to add formatting such as bold or italics to the text in your comments.

To view the Properties bar, do one of the following:

- Right-click the toolbar area; choose Properties Bar.
- Press [Ctrl-E]



- A. Insert Text tool
- B. Replace Text tool
- C. Delete Text tool
- D. Sticky Note tool
- E. Text Correction Markup tool



6. Inserting symbols or special characters

An 'insert symbol' feature is not available for annotations, and copying/pasting symbols or non-keyboard characters from Microsoft Word does not always work. Use angle brackets < > to indicate these special characters (e.g., <alpha>, <beta>).

7. Editing near watermarks and hyperlinked text

eProof documents often contain watermarks and/or hyperlinked text. Selecting characters near these items can be difficult using the mouse alone. To edit an eProof which contains text in these areas, do the following:

- Without selecting the watermark or hyperlink, place the cursor near the area for editing.
- Use the arrow keys to move the cursor beside the text to be edited.
- Hold down the shift key while simultaneously using arrow keys to select the block of text, if necessary.
- Insert, replace, or delete text, as needed.

8. Summary of main functions

- A. Insert text - Use Insert Text tool (position cursor and begin typing)
- B. Replace text - Use Replace Text tool (select text and begin typing)
- C. Delete text - Use Strikethrough Text tool (select text and press delete key)
Note: The Text Correction Markup tool combines the functions of all three tools.
- D. Sticky Note - Use Sticky Note tool to add comments not related to text correction.

9. Reviewing changes

To review all changes, do the following:

- Click the Comments button to reveal the comment tools
- Click the triangle next to Comments List (if not already visible)

Note: Selecting a correction in the list will highlight the corresponding item in the document, and vice versa.

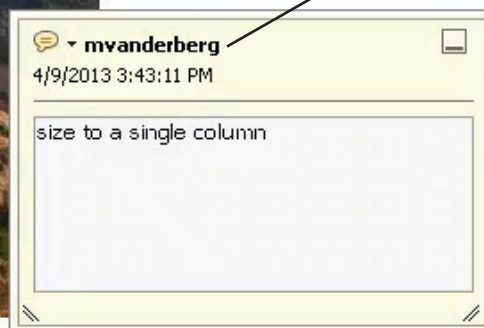
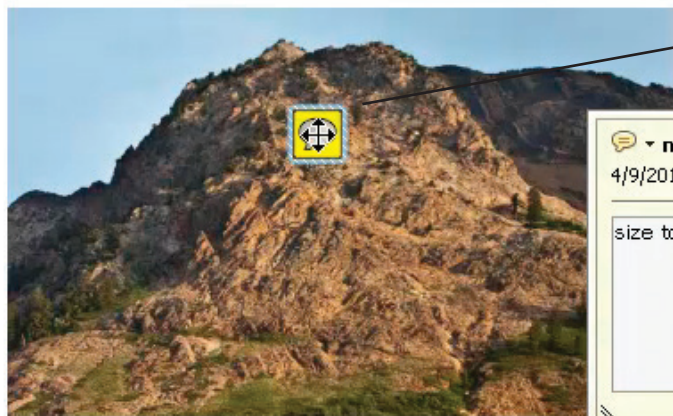
10. Still have questions?

Try viewing our brief training video at <https://authorcenter.dartmouthjournals.com/Article/PdfAnnotation>

This PDF needs to be proofread and annotated.

Note: these annotations will not actually change the content of the PDF – they just point out the areas where corrections are needed. The actual corrections will be made to the native article files.

1. **Insert Text Tool:** Text needs inserted into this sentence.
2. **Replace Text Tool:** Some of the text in this paragraph needs to be replaced.
3. **Delete Text Tool:** Some of the text in this overly long sentence needs to be deleted.
4. **Sticky Note Tool:** This image needs to be reduced:



A

B

C

D

CD4⁺ Group 1 Innate Lymphoid Cells (ILC) Form a Functionally Distinct ILC Subset That Is Increased in Systemic Sclerosis

Florence Roan,^{*,†,1} Thomas A. Stoklasek,^{*,1} Elizabeth Whalen,^{*} Jerry A. Molitor,[‡] Jeffrey A. Bluestone,[§] Jane H. Buckner,^{*} and Steven F. Ziegler^{*}

Innate lymphoid cells (ILC) are a heterogeneous group of cellular subsets that produce large amounts of T cell–associated cytokines in response to innate stimulation in the absence of Ag. In this study, we define distinct patterns of surface marker and cytokine expression among the ILC subsets that may further delineate their migration and function. Most notably, we found that the subset previously defined as group 1 ILC (ILC1) contains CD4⁺ CD8[−], CD4[−] CD8⁺, and CD4[−] CD8[−] populations. Although all ILC1 subsets shared characteristics with Th1 cells, CD4⁺ ILC1 also demonstrated significant phenotypic and functional heterogeneity. We also show that the frequencies of CD4⁺ ILC1 and NKp44⁺ group 3 ILC, but not CD4[−] ILC1 or group 2 ILC, are increased in the peripheral blood of individuals with systemic sclerosis (SSc), a disease characterized by fibrotic and vascular pathology, as well as immune dysregulation. Furthermore, we demonstrate that CD4⁺ and CD4[−] ILC1 are functionally divergent based on their IL-6R α expression and that the frequency of IL-6R α expression on ILC is altered in SSc. The distinct phenotypic and functional features of CD4⁺ and CD4[−] ILC1 suggest that they may have differing roles in the pathogenesis of immune-mediated diseases, such as SSc. *The Journal of Immunology*, 2016, 196: 000–000.

Innate lymphoid cell (ILC) subsets that mirror Th cells in their effector cytokine profiles have recently emerged as central players in homeostatic and inflammatory conditions. Long-lived tissue-resident group 2 ILC (ILC2) constitutively produce IL-5 and play varied roles in maintaining immune and metabolic homeostasis (1–4); group 3 ILC (ILC3) maintain the integrity of the intestinal barrier, in part through production of IL-22 (5, 6). ILC2 and ILC3 can also express MHC class II and may act as APCs in the initiation of inflammation or in the maintenance of tolerance (7–10). In keeping with the functional parallels between ILC and Th cell subsets, group 1 ILC (ILC1) appear to be important in coordinating type 1 inflammatory responses (11, 12),

ILC2 are required in numerous models of type 2 immunity (13–16), whereas ILC3, like Th17 and Th22 cells, are central players in IL-17– and/or IL-22–driven inflammation (17, 18).

In human studies, alterations in ILC frequencies in a number of diseases suggest that these innate populations may play key roles in the pathogenesis of human autoimmunity (19–27). How ILC subsets affect disease susceptibility, development, and progression remains undefined. However, in multiple sclerosis and psoriasis, treatments that decreased patients' clinical severity scores also correlated with normalization of ILC frequencies (19, 21, 27). In psoriasis, increased frequencies of NKp44⁺ ILC3 during active disease, as well as normalization of these frequencies with treatment, occurred in the skin and peripheral blood. These studies indicate that systemic alterations in ILC subsets occur in autoimmunity and may present an important target for disease therapy. The regulation and function of these ILC populations, as well as the degree to which they parallel or differ from T cells, may have significant implications for the efficacy and side effect profile of novel therapeutic approaches.

We performed a comprehensive analysis of human peripheral blood ILC subsets and describe novel ILC1 populations that express CD4 and CD8 α . Although these newly described ILC1 populations shared some characteristics with Th1 cells, CD4⁺ ILC1, in particular, were potent producers of TNF- α , GM-CSF, and IL-2 and showed considerable diversity in their chemokine and cytokine receptor expression. Our data illustrate that ILC1 cannot be thought of simply as innate equivalents of Th1 cells. We also show that peripheral blood CD4⁺, but not CD4[−], ILC1 frequencies are altered in systemic sclerosis (SSc), a complex and poorly understood autoimmune disease characterized by fibrotic and vascular pathology. These data demonstrate a previously unappreciated heterogeneity in human peripheral blood ILC1 and suggest a role for ILC in the pathogenesis of SSc.

*Benaroya Research Institute at Virginia Mason, Seattle, WA; [†]Division of Allergy and Infectious Diseases, University of Washington, Seattle, WA; [‡]Division of Rheumatology, University of Minnesota, Minneapolis, MN; and [§]Diabetes Center, University of California San Francisco, San Francisco, CA

¹F.R. and T.A.S. contributed equally to this work.

ORCID: 0000-0001-8793-7848 (J.A.B.).

Received for publication July 2, 2015. Accepted for publication January 1, 2016.

This work was supported in part by the Crohn's and Colitis Foundation of America (to F.R.), the Juvenile Diabetes Research Foundation Cooperative Center for Cell Therapy (to J.A.B. and S.F.Z.), the Merck Scleroderma Research Fund at Benaroya Research Institute (to F.R. and S.F.Z.), and National Institutes of Health Grants T32AR056969 (to T.A.S.) and UL1TR000423 (to S.F.Z.).

The sequences presented in this article have been submitted to the National Center for Biotechnology Information Gene Expression Omnibus under accession number GSE69596.

Address correspondence and reprint requests to Dr. Steven F. Ziegler, Immunology Program, Benaroya Research Institute at Virginia Mason, 1201 9th Avenue, Seattle, WA 98101. E-mail address: sziegler@benaroyaresearch.org

The online version of this article contains supplemental material.

Abbreviations used in this article: BRI, Benaroya Research Institute; CLA, cutaneous lymphocyte Ag; cRPMI, complete RPMI; DN, double negative; Eomes, eomesodermin; HS, human serum; ILC, innate lymphoid cell; ILC1, group 1 ILC; ILC2, group 2 ILC; ILC3, group 3 ILC; MFI, mean fluorescence intensity; RNAseq, RNA sequencing; RT, room temperature; SSc, systemic sclerosis.

Copyright © 2016 by The American Association of Immunologists, Inc. 0022-1767/16/\$30.00

Materials and Methods

Abs and reagents

Abs used for flow cytometric analyses and cell sorting included the following: CCR10 PE (6588-5), CD117 (104D2) BV421/BV605/PE-Cy7, CD11c (3.9) FITC, CD123 (6H6) FITC, CD126 (UV4) biotin, CD127 (A019D5) BV650, CD130 (AM64) PE, CD14 (HCD14) FITC, CD16 (3G8) FITC/BV421, CD27 (O323) biotin, CD28 (CD28.2) BV421, CXCR3 (G025H7) BV421/PE-Cy7, CXCR5 (J252D4) BV421, CD19 (HIB19) FITC, CCR4 (L291H4) PerCP-Cy5.5/A647, CCR5 (HEK1/85a) A647, CCR6 (G034E3) BV605, CCR7 (G043H7) BV421, CRTH2 (BM16) PerCP-Cy5.5/A647/BV421, CCR9 (L053E8) A647, CD3 (UCHT1) A700/BV421/FITC, NKp44 (P44-8) PE, CD34 (581) FITC, CD4 (OKT4) A700/BV605/BV785, CD45 (HI30) BV510, CD45RO (UCHL1) A700, CD45RA (HI100) BV421, CD56 (HCD56) A700/BV605, CD62L (DREG-56) PE, CD8 α (RPA-T8) A700, CD94 (DX22) FITC, cutaneous lymphocyte Ag (CLA; HECA-452) biotin, Fc ϵ RI α (AER-37) FITC, GATA3 (TWAJ) PE, GM-CSF (BVD2-21C11) PE, granzyme A (CB9) A700, granzyme B (GB11) A647, IFN- γ (4S.B3) BV785, IL-13 (JES10-5A2) PE, IL-17A (BL168) A647, IL-2 (MQ1-17H12) A647, IL-22 (22URTI) PE-Cy7, TNF- α (Mab11) PE-Cy7, perforin (dG9) PE, T-bet (4B10) A647/PE-Cy7, and TCR α (IP26) PE (all from BioLegend); CD117 (104D2) PE-Cy7, CD2 (RPA-2.10) allophycocyanin, CD45 (HI30) e450, eomesodermin (Eomes; WD1928) PE, and Fixable Viability Dye eFluor 780 (all from eBioscience); and streptavidin PE and PE-Cy7, phospho-STAT1 (4a) PE, and phospho-STAT3 (4P-STAT3) PerCP-Cy5.5 (all from BD Biosciences).

Complete RPMI medium (cRPMI) used for stimulations and resuspension included RPMI 1640 (Sigma), 50 U/ml penicillin/50 μ g/ml streptomycin, 10 mM HEPES, 1 mM sodium pyruvate, 1 \times MEM NEAA, 2 mM L-glutamine (all from Life Technologies), and 1 or 10% human serum (HS; Omega Scientific). FACS buffer included 1 \times PBS/1% BSA (w/v) with or without 0.5% sodium azide (w/v) (both from Sigma). MACS buffer was composed of 1 \times HBSS (HyClone)/5% FBS (Sigma)/20 mM HEPES/Pen-Strep/2 mM EDTA (Sigma). Sort buffer included 1 \times HBSS/2.5% FCS/Pen-Strep/20 mM HEPES.

Human subjects

Fresh whole blood and frozen PBMC from control subjects were obtained from healthy individuals who were participants in the Benaroya Research Institute (BRI) Healthy Control Registry and Biorepository without a self-reported personal history of autoimmunity. Matched controls that were compared with SSc patients also did not have a self-reported family history of autoimmunity. Frozen PBMC from SSc patients were obtained from subjects in the BRI Rheumatic Diseases Registry and Biorepository. Control and SSc cohorts were matched for age and gender in all studies. Frozen cord blood cell samples were from subjects in the BRI Control Biorepository. Protocols for the collection and use of samples in the BRI registries and Biorepositories were reviewed and approved by the BRI Institutional Review Board.

Isolation of PBMC

Human PBMC were isolated from peripheral blood by centrifugation over a Ficoll-Paque Plus (GE Healthcare) gradient. Previously frozen PBMC were quick thawed; prewarmed cRPMI with 10% HS and then 1% HS were added drop-wise to wash the cells.

Cell staining, flow cytometry, and cell sorting

Cells were stained with Fixable Viability Dye eFluor 780 (eBioscience) and then stained for surface markers for 25 min at room temperature (RT). Cells were then fixed with 2% paraformaldehyde (EMS)/PBS for 20 min at 4°C or fixed and permeabilized for intracellular/intranuclear staining. For intracellular cytokine staining, cells were permeabilized using BD Cytofix/Cytoperm, according to the manufacturer's instructions, and then stained in 1 \times BD Fix/Perm buffer for 25 min at RT. For intranuclear staining, cells were fixed with 4% paraformaldehyde for 10 min at RT and permeabilized with ice-cold (-20°C) methanol (Sigma) for 15 min on ice. Intranuclear staining was then performed in Foxp3 buffer (eBioscience) for 45 min at RT. All flow cytometry data were acquired on a BD LSR II or BD Fortessa, and analyses were performed using FlowJo v10.

For cell sorting, freshly isolated PBMC were lineage depleted with FITC-conjugated Ab (anti-CD3, CD14, CD19, CD16, CD94, CD11c, CD123) and anti-FITC beads (Miltenyi Biotec), according to the manufacturer's instructions, with minor modifications. Twenty microliters of beads/10⁷ cells were used in most experiments. After staining with viability dye and surface markers, cells were sorted on a BD FACSAria II using a 70- μ m nozzle and collected into Eppendorf tubes containing cRPMI/10% HS.

In vitro cultures

CD4⁺ and CD4⁻ ILC1 were sorted from freshly isolated PBMC as described above, and ~10,000 cells were added to a single well in a 96-well round-bottom plate coated with irradiated mouse embryonic fibroblasts (R&D Systems) and cultured for 7 d in cRPMI/10% HS with 20 ng/ml IL-2 (BioLegend) and 20 ng/ml IL-7 (BioLegend). Cells were stained with Fixable Viability Dye eFluor 780 (eBioscience) and then stained for surface markers and analyzed by flow cytometry.

rIL-6 and PMA/ionomycin stimulation

Stimulations were performed with 5 ng/ml rIL-6 (BioLegend) in cRPMI at 37°C/5% CO₂ for 20 min after a 30-min rest (10 \times 10⁶ cells/ml in cRPMI/1% HS; 37°C/5% CO₂) and staining with viability dye and surface markers. PMA/ionomycin stimulations were performed in cRPMI/10% HS with 50 ng/ml PMA (Sigma), 750 ng/ml ionomycin (Sigma), and 10 μ g/ml brefeldin A (Sigma) for 6 h at 37°C/5% CO₂.

RNA sequencing

ILC subsets were sorted as described above, and 2000 cells from each population were used to prepare cDNA using a SMARTer Ultra Low RNA Kit v2 (Clontech). A Nextera XT kit was used for library construction, and sequencing was performed on an Illumina HiSeq2500. Analysis was performed using the R package, DESeq2, and a false-discovery rate < 0.05 was considered significant. The sequences presented in this article have been submitted to the National Center for Biotechnology Information Gene Expression Omnibus under accession number GSE69596.

Statistics

Statistical analyses were performed using Prism with the two-tailed unpaired Mann-Whitney test. The *p* values < 0.05 were considered significant.

Results

CD4⁺, CD8⁺, and double-negative populations are present in peripheral blood ILC1

Like their Th1, Th2, and Th17/Th22 Th cell counterparts, ILC subsets are categorized based on their expression of specific transcription factors and effector cytokines: ILC1 express T-bet and IFN- γ ; ILC2 express GATA-3 and type 2 effector cytokines, such as IL-13 and IL-5; and ILC3 express ROR γ t and the cytokines IL-22 and/or IL-17 (28). Under this nomenclature, NK cells and lymphoid tissue inducers are considered ILC1 and ILC3, respectively. To better define the relative frequencies of ILC1, ILC2, and ILC3 in human peripheral blood, we first characterized the overall composition of ILC subsets by flow cytometry in a cohort of healthy subjects. Our gating strategy for the identification of peripheral blood ILC is shown in Fig. 1A. Although all ILC subsets express CD127 (IL-7R α) but are negative for lineage-specific surface markers for T cells, B cells, monocytes, and dendritic cells, they can be further divided into groups by their differential expression of c-kit and CRTH2. Only ILC2 express CRTH2; within the CRTH2⁻ population, ILC1 are c-kit⁻, whereas ILC3 are c-kit⁺. In control subjects, very few peripheral blood ILC3 express NKp44. To exclude mature NK cells, we gated on CD56⁻ ILC1 in our analyses (29). Lack of expression of CD16, perforin, and granzyme B in CD56⁻ ILC1 further confirmed that these cells are distinct from mature NK cells (Supplemental Fig. 1), consistent with previous reports for ILC1 (29, 30). We were surprised to find that the peripheral blood ILC1 compartment contained CD4⁺ CD8⁻, CD4⁻ CD8⁺, and CD4⁻ CD8⁻ populations (referred to as CD4⁺, CD8⁺, and double-negative [DN] ILC1, respectively), whereas the ILC2 and ILC3 subsets did not express CD4 or CD8 α (Fig. 1B). Although ILC subset frequencies varied considerably within a cohort of healthy controls (Table I), ILC frequencies were stable within an individual over time (Supplemental Fig. 2A). CD4⁺ ILC1 constituted more than half of peripheral blood ILC1 in the majority of healthy controls. In addition, ILC subset fre-

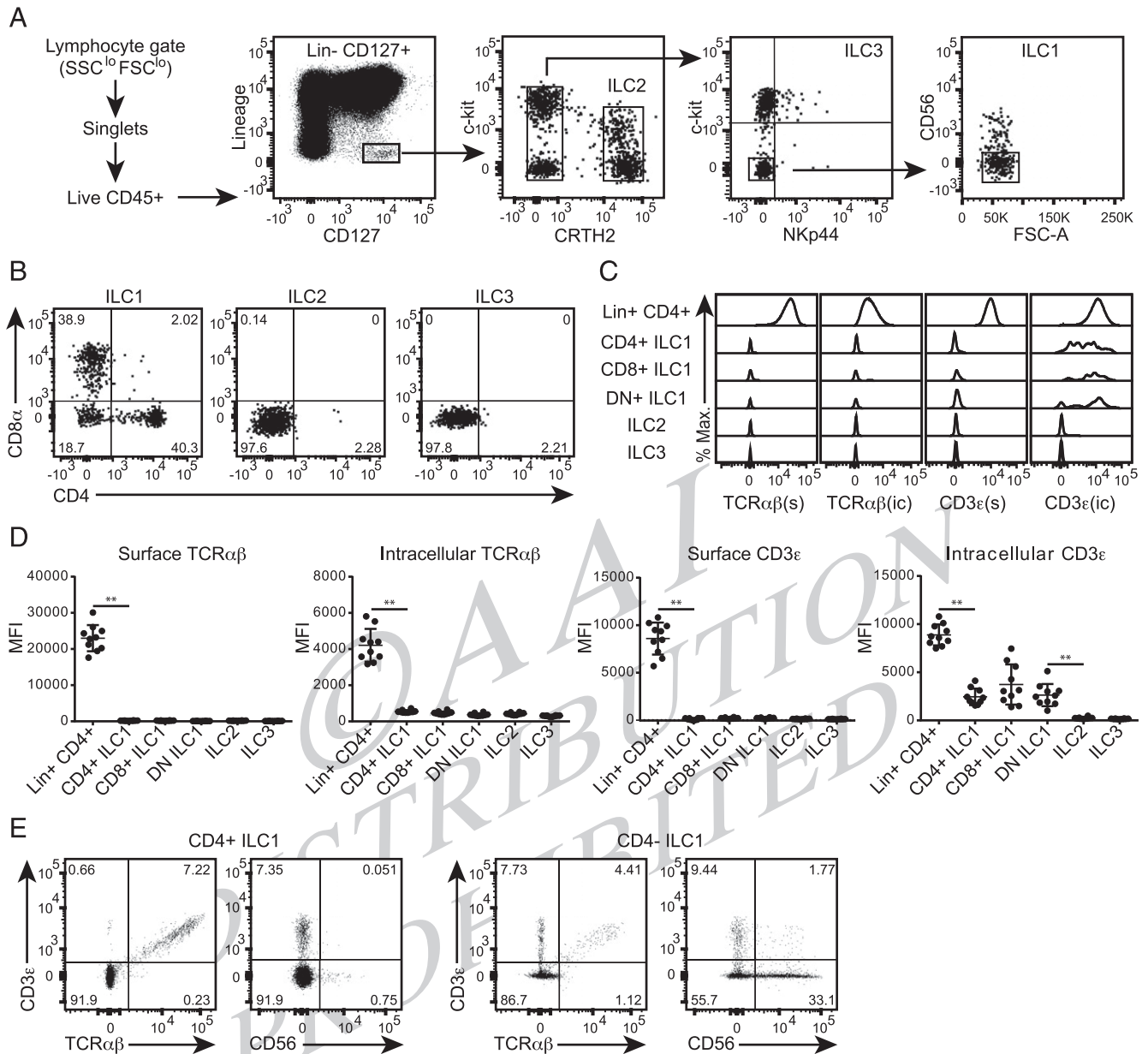


FIGURE 1. CD4⁺, CD8⁺, and DN populations in the ILC1 subset. **(A)** Gating for peripheral blood ILC subsets: after gating on lymphocytes (FSC^{low} SSC^{low}), singlets, and live CD45⁺ cells, total ILC were defined as Lin⁻ CD127⁺. Lineage markers included CD3e, CD19, CD14, CD123, CD11c, FcεRIα, CD34, CD94, ± CD16. Within total ILC, ILC2 were defined as CRTH2⁺, ILC1 were defined as CRTH2⁻ c-kit⁻ CD56⁻, and ILC3 were defined as CRTH2⁻ c-kit⁺. A small fraction of ILC3 was NKp44⁺. **(B)** ILC subsets in fresh and frozen PBMC from control subjects were assessed for expression of CD4 and CD8α. Flow plots are from a single representative individual (*n* > 20). **(C)** ILC subsets from fresh and frozen PBMC were assessed for surface (s) and intracellular (ic) TCRαβ and CD3ε. CD3ε was also included in the lineage markers in these analyses. **(D)** TCRαβ and CD3ε MFI in ILC subsets (*n* = 10). **(E)** Sorted CD4⁺ and CD4⁻ ILC1 populations were cultured with irradiated feeder cells, IL-2, and IL-7 for 7 d. Live cells were analyzed for surface expression of CD3ε, TCRαβ, and CD56 by flow cytometry. Flow plots are from a single individual (*n* = 2). ***p* < 0.0001, two-tailed unpaired Mann-Whitney test.

quencies from fresh PBMC were comparable to frequencies following freeze-thawing (Supplemental Fig. 2B).

Further examination of ILC1 revealed that, like a recently described CD4⁺ CD3⁻ innate-like T cell population (31), CD4⁺ ILC1 expressed intracellular CD3ε, although we detected little or no expression of surface or intracellular TCRαβ on any peripheral blood ILC (Fig. 1C, 1D). Furthermore, intracellular CD3ε was present in CD4⁺ ILC1, as well as in a large percentage of all ILC1 subsets, but not in ILC2 or ILC3.

We next evaluated surface CD3ε and TCRαβ expression on sorted CD4⁺ and CD4⁻ ILC1 after a 7 d culture with irradiated feeder cells, IL-2, and IL-7 (Fig. 1E). The vast majority of sorted

cells remained CD3ε⁻ and TCRαβ⁻, indicating that they are not activated T cells or NKT cells with low expression of TCR. A small percentage of CD3ε⁺ TCRαβ⁺ cells were present in both CD4⁺ and CD4⁻ ILC1 cultures, although it is unclear whether there was preferential expansion or survival of a small number of contaminating T lymphocytes or whether some ILC1 can indeed upregulate surface CD3 and TCR. It is interesting to note that a small percentage of cultured CD4⁻ ILC1 expressed surface CD3ε in the absence of TCRαβ. In addition, a fraction of CD4⁻ ILC1 upregulated CD56 postculture, suggesting that this marker may not distinguish between conventional NK cells and other ILC1.

287
288
289
290
291
292
293
294
295
296
297
298
299
300
301
302
303
304
305
306
307
308
309
310
311
312
313
314
315
316
317
318
319
320
321
322
323
324
325
326
327
328
329
330
331
332
333
334
335
336
337
338
339
340
341
342
343
344
345
346
347
348
349
350

Table I. Composition of peripheral blood ILC

Subset	Frequency (%; Mean \pm SD [Range])
Within Total Live CD45 ⁺ Lymphocytes	
Total ILC	0.08 \pm 0.05 (0.02–0.24)
Within Total ILC (Lin ⁻ CD127 ⁺)	
ILC1	21.7 \pm 12.2 (5.2–71.8)
ILC2	31.7 \pm 14.1 (4.7–57.0)
ILC3	33.9 \pm 14.4 (7.8–64.5)
NKp44 ⁺ ILC3	2.5 \pm 2.7 (0.3–13.7)
CD4 ⁺ ILC1	12.3 \pm 6.2 (5.7–25.8)
CD4 ⁻ ILC1	7.4 \pm 3.0 (2.9–13.3)

ILC subset frequencies were determined by flow cytometry from previously frozen PBMC of healthy control subjects ($n = 39$ for total ILC, ILC1, ILC2, ILC3 and NKp44⁺ ILC3; $n = 20$ for CD4⁺ and CD4⁻ ILC1).

These data demonstrate that the ILC1 subset contains distinct populations characterized by CD4 and CD8 α surface expression, though the shared expression of intracellular CD3 ϵ in ILC1 suggests a lineage relationship among the ILC1 populations that may be distinct from ILC2 and ILC3.

CD4⁺ ILC1 demonstrate phenotypic and functional heterogeneity, although all ILC1 subsets share features with CD4⁺ Th1 cells

Effectors of type 1 inflammation, such as CD4⁺ Th1 cells, CD8⁺ T cells, and NK cells, are characterized by IFN- γ production, expression of the chemokine receptor CXCR3, and expression of the transcription factors T-bet and Eomes (32–35). To examine whether all ILC1 populations shared a type 1 phenotype, we first delineated the expression of T-bet and Eomes and contrasted this with the expression of the Th2-associated factor GATA-3 by flow cytometry. As expected, GATA-3 was expressed in ILC2 but was low or absent in ILC1 and ILC3 (Fig. 2A). Although CD4⁺ ILC1_{F2} expressed T-bet, but not Eomes, CD4⁻ ILC1 coexpressed Eomes and T-bet, most prominently in the CD8⁺ ILC1 population (Fig. 2B, 2C). All ILC1 subsets also expressed CXCR3, although CD8⁺ ILC1 contained the highest percentage of CXCR3⁺ cells (Fig. 2B, 2C).

To evaluate cytokine production from ILC1, we sorted ILC subsets from control subjects and analyzed intracellular cytokine production after PMA/ionomycin stimulation by flow cytometry. CD8⁺ and DN ILC1 were analyzed together as CD4⁻ ILC1 because of the lower frequency of these cells compared with CD4⁺ ILC1 in most individuals and the dominant Th1-type phenotype in both of these populations. CD4⁺ and CD4⁻ ILC1 produced IFN- γ but little or no IL-13, IL-17A, or IL-22 (Fig. 3A). Within CD4⁺ F3

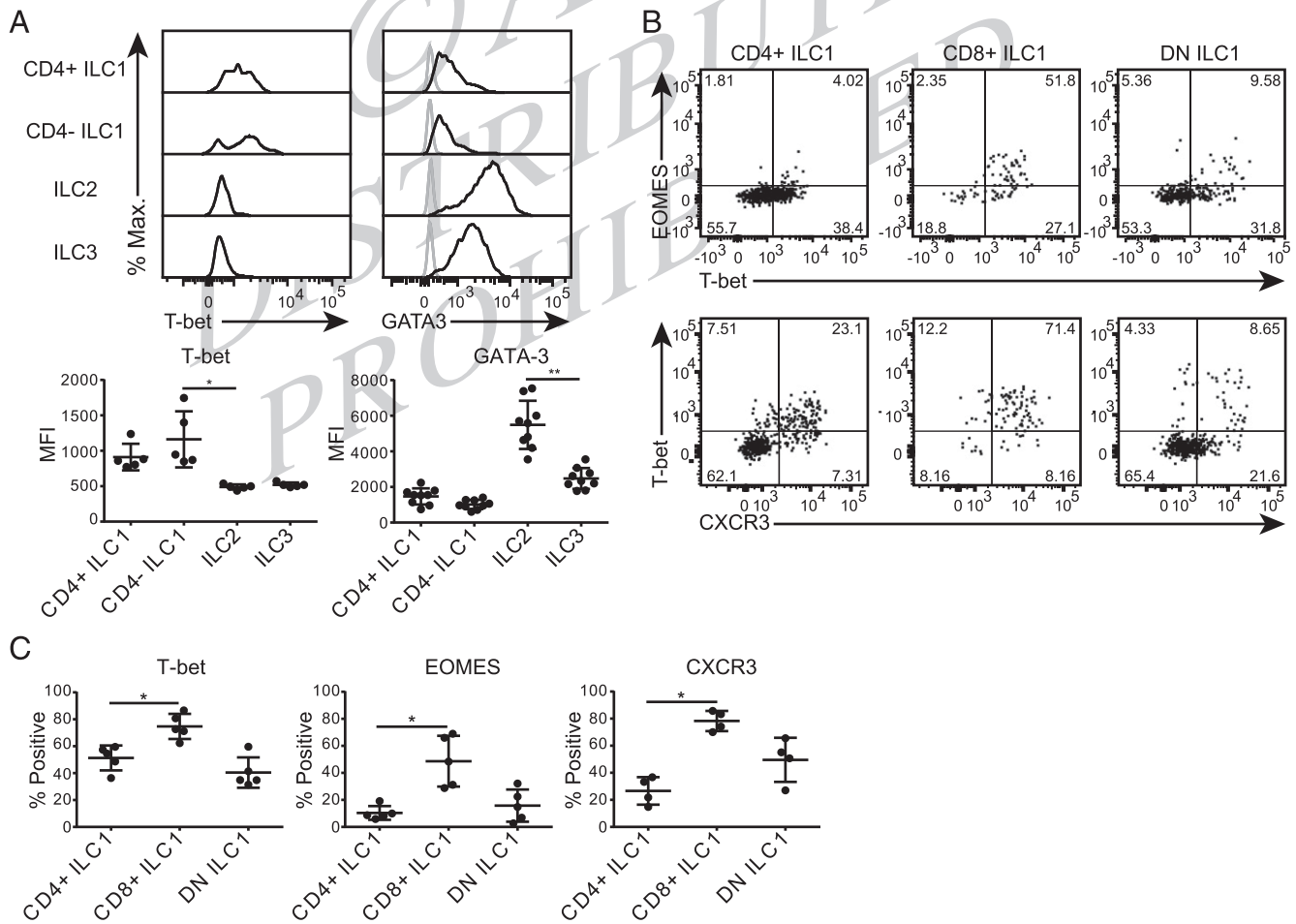


FIGURE 2. Gradient of Th1 phenotype in ILC1 subsets. ILC subsets in fresh or frozen PBMC from control subjects were analyzed for transcription factor and CXCR3 expression. **(A)** T-bet and GATA-3 expression in ILC subsets (gray line = isotype control; black line = transcription factor). Graphs show representative staining from $n = 5-9$ subjects. **(B)** T-bet, Eomes, and CXCR3 expression in CD4⁺, CD8⁺, and DN ILC1 by flow cytometry. Flow plots are from a single representative individual from a total of $n = 5-9$ subjects for each stain set. **(C)** Frequency of T-bet⁺, Eomes⁺, and CXCR3⁺ cells in CD4⁺, CD8⁺, and DN ILC1 ($n = 4-5$). * $p < 0.05$, ** $p < 0.0001$, two-tailed unpaired Mann-Whitney test.

415
416
417
418
419
420
421
422
423
424
425
426
427
428
429
430
431
432
433
434
435
436
437
438
439
440
441
442
443
444
445
446
447
448
449
450
451
452
453
454
455
456
457
458
459
460
461
462
463
464
465
466
467
468
469
470
471
472
473
474
475
476
477
478

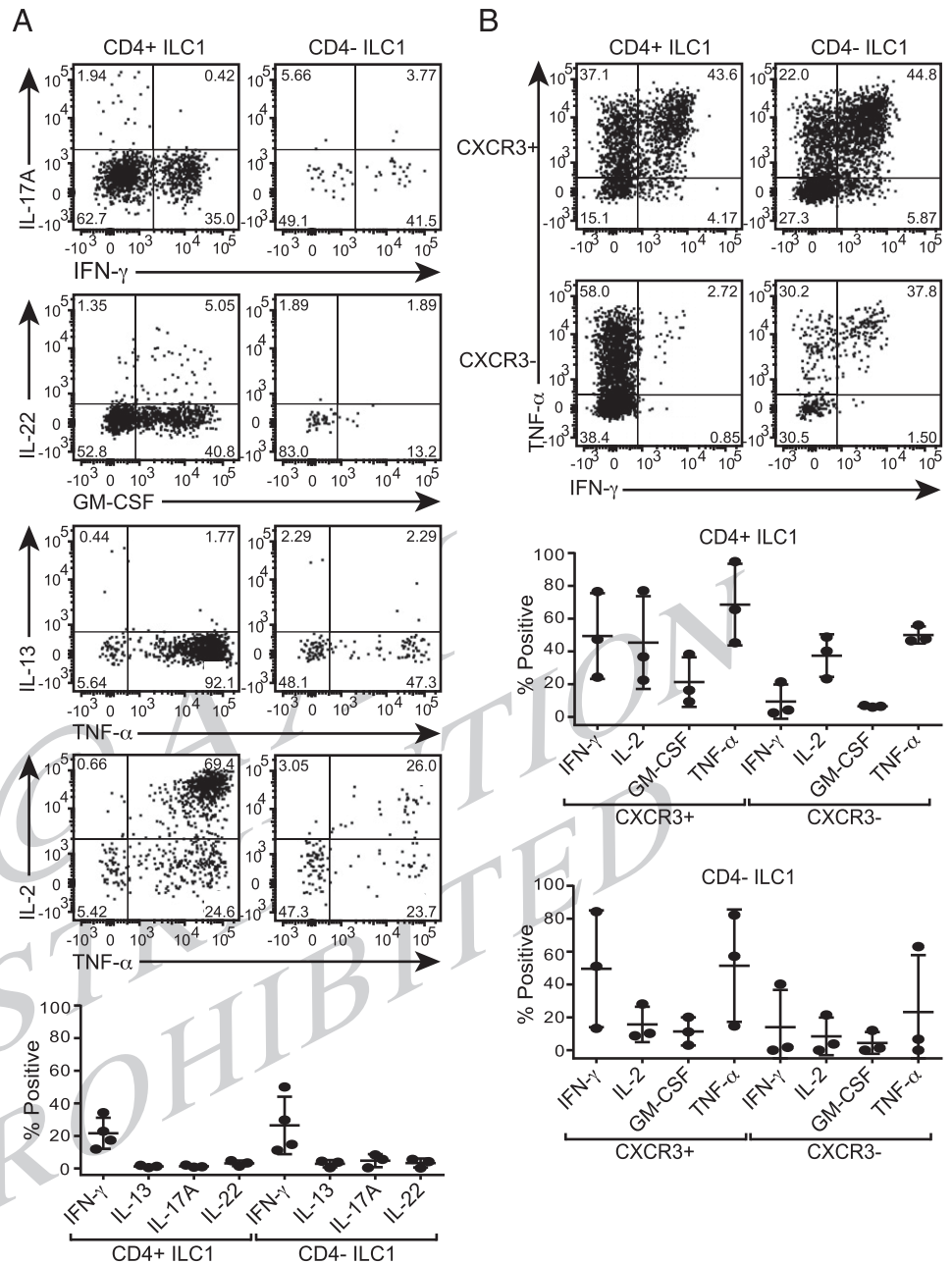


FIGURE 3. CD4⁺ and CD4⁻ ILC1 cytokine production. Fresh PBMC were prepared from peripheral blood, lineage depleted using a MACS column, stained for ILC surface markers, and flow sorted for CD4⁺ and CD4⁻ ILC1 subsets (*n* = 3) (A) or CXCR3⁺ and CXCR3⁻ populations within the CD4⁺ and CD4⁻ ILC1 subsets (*n* = 3) (B). The sorted populations were stimulated with PMA/ionomycin/brefeldin A for 6 h and then examined for intracellular cytokine expression by flow cytometry.

ILC1, IFN- γ production was largely restricted to CXCR3⁺ cells (Fig. 3B). CD4⁺ ILC1 were also potent producers of TNF- α , GM-CSF, and IL-2 (Fig. 3). To varying degrees, all other ILC subsets were also capable of producing TNF- α , GM-CSF, and IL-2 poststimulation (Fig. 3, Supplemental Fig. 3). Effector cytokine expression in peripheral blood ILC2 and ILC3 was consistent with previous reports (Supplemental Fig. 3) (30).

Although the CD4⁺, CD8⁺, and DN ILC1 populations that we describe shared numerous features with Th1 cells, CD4⁺ ILC1 expressed lower levels of Th1-associated factors than did CD4⁻ ILC1 and showed substantial functional heterogeneity. Coexpression of T-bet and Eomes in CD8⁺ ILC1 suggests that this subset shares more similarities with NK cells than do other ILC1 subsets. These data indicate that ILC1, particularly CD4⁺ ILC1, do not fit strictly into a Th1 paradigm.

ILC subsets are characterized by differential surface marker expression

Because CD4⁺ ILC1 demonstrated phenotypic and functional characteristics distinct from CD4⁻ ILC1 and had a lower frequency of cells expressing the Th1-associated factors T-bet, CXCR3, or IFN- γ , we were interested in whether chemokine receptors and activation markers might be able to further define functionally distinct CD4⁺ ILC1 populations. Differential patterns of chemokine receptor expression are important in determining lymphocyte migration to specific tissues and lymph nodes, and they can also be used to identify specific T cell subsets (36–42). Therefore, to provide some insight into potential functional differences among these ILC subsets, we performed a detailed examination of ILC chemokine receptor expression profiles (Fig. 4A, Table II).

Consistent with a Th1 phenotype, ILC1 had the highest frequency of CXCR3-expressing cells; however, CD4⁺ ILC1, which had a lower frequency of CXCR3⁺ cells than CD4⁻ ILC1, dem-

479
480
481
482
483
484
485
486
487
488
489
490
491
492
493
494
495
496
497
498
499
500
501
502
503
504
505
506
507
508
509
510
511
512
513
514
515
516
517
518
519
520
521
522
523
524
525
526
527
528
529
530
531
532
533
534
535
536
537
538
539
540
541
542
543
544
545
546
547
548
549
550
551
552
553
554
555
556
557
558
559
560
561
562
563
564
565
566
567
568
569
570
571
572
573
574
575
576
577
578
579
580
581
582
583
584
585
586
587
588
589
590
591
592
593
594
595
596
597
598
599
600
601
602
603
604
605
606

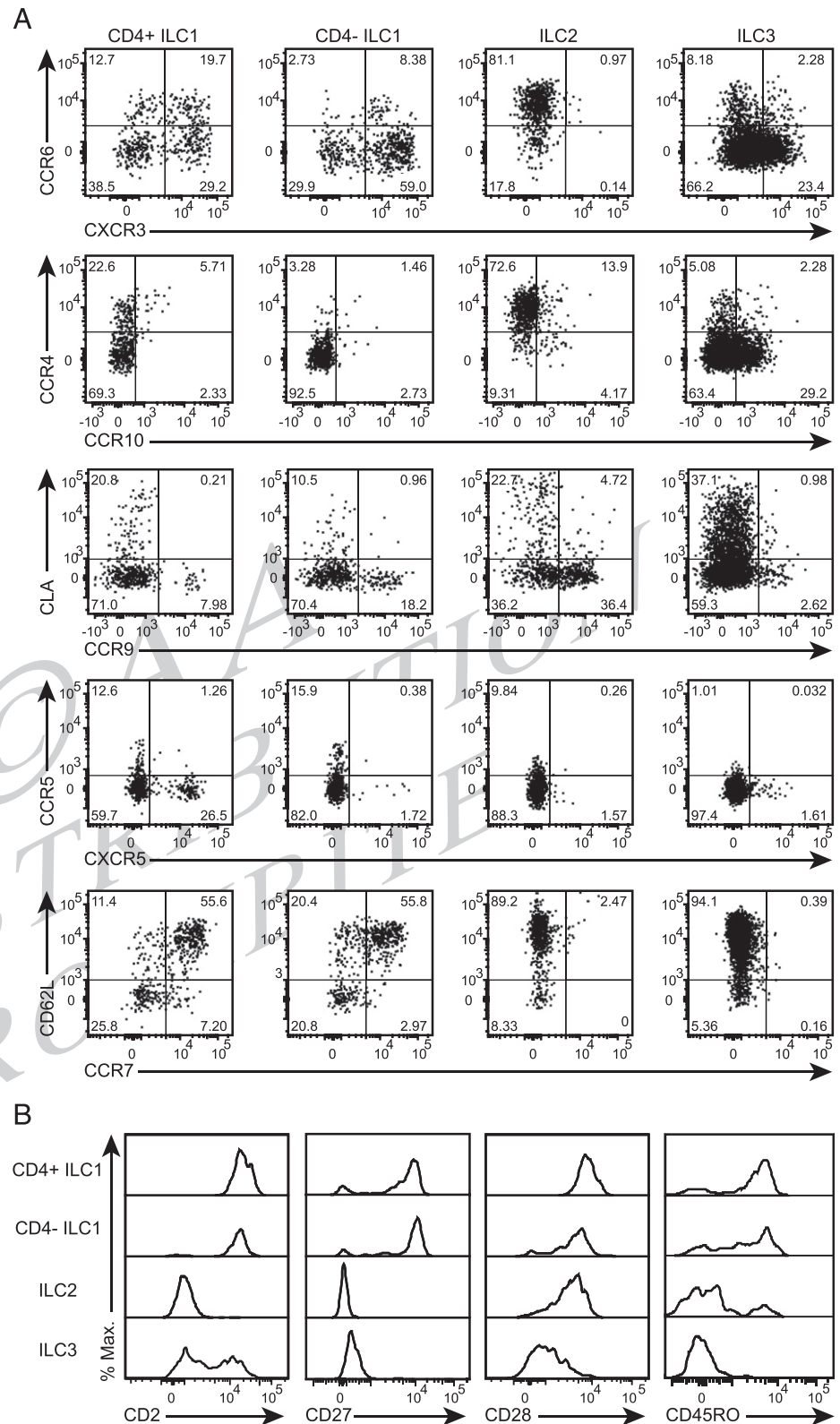


FIGURE 4. Distinct chemokine receptor and costimulatory marker expression on ILC subsets. **(A)** Fresh PBMC from control subjects were isolated from peripheral blood and rested for 1 h at 37°C/5% CO₂ and chemokine receptor expression was analyzed on ILC subsets by flow cytometry. Flow plots are from a single representative individual ($n = 5-7$). **(B)** ILC subsets from fresh or frozen PBMC were examined for their activation marker and CD45RO expression by flow cytometry. Flow plots are from a single representative individual ($n > 10$).

onstrated the highest level of heterogeneity in chemokine receptor expression. A higher frequency of CD4⁺ ILC1 than CD4⁻ ILC1 expressed CLA, a skin-homing receptor, and a significant percentage of CD4⁺, but not CD4⁻, ILC1 expressed CCR4, CCR10, and CXCR5. Of particular note, the coexpression of CCR7 and CD62L on a high frequency of all ILC1 populations distinguished ILC1 from ILC2 and ILC3, which expressed CD62L but not CCR7.

ILC2, like Th2 cells, were nearly all CCR4⁺. ILC2 also had the highest frequency of cells positive for CCR4, CCR6, and CCR9, chemokine receptors important in homing to barrier surfaces of the skin, lung, and gut (43, 44). ILC3 were very heterogeneous in their chemokine receptor expression; however, other than CD62L, CLA was the most frequently expressed surface receptor on ILC3 of the chemokine receptors and adhesion molecules examined.

671
672
673
674
675
676
677
678
679
680
681
682
683
684
685
686
687
688
689
690
691
692
693
694
695
696
697
698
699
700
701
702
703
704
705
706
707
708
709
710
711
712
713
714
715
716
717
718
719
720
721
722
723
724
725
726
727
728
729
730
731
732
733
734

Table II. Peripheral blood ILC surface marker expression

Surface Marker	CD4 ⁺ ILC1	CD4 ⁻ ILC1	ILC2	ILC3
CCR6	30.4 ± 9.4 (17.3–44.1)	18.5 ± 6.6 (7.9–26.2)	58.7 ± 14.4 (43.1–83.7)	20.0 ± 7.3 (12.8–28.7)
CXCR3	39.9 ± 9.3 (24.9–51.9)	66.8 ± 7.4 (53.3–74.5)	0.8 ± 0.5 (0.3–1.8)	34.1 ± 18.3 (14.3–65.5)
CCR4	39.0 ± 12.0 (24.4–62.2)	7.6 ± 3.3 (4.5–14.1)	78.4 ± 8.3 (64.6–88.9)	12.8 ± 5.8 (6.9–21.3)
CCR10	17.6 ± 11.4 (6.3–41.4)	5.3 ± 2.1 (3.5–9.7)	8.6 ± 5.6 (3.5–19.5)	29.3 ± 10.1 (14.6–43.7)
CLA	29.2 ± 15.7 (17.0–54.3)	17.5 ± 6.3 (11.6–28.2)	26.0 ± 9.7 (15.6–39.1)	39.3 ± 10.8 (25.7–52.8)
CCR9	7.4 ± 3.4 (2.1–11.7)	15.5 ± 4.7 (10.3–21.7)	30.0 ± 9.7 (17.0–41.1)	5.8 ± 1.9 (3.6–9.0)
CCR5	8.2 ± 3.8 (3.5–14.1)	21.0 ± 12.4 (6.2–37.5)	10.7 ± 8.9 (5.78–28.6)	1.9 ± 1.5 (0.4–4.5)
CXCR5	15.8 ± 7.1 (8.1–27.9)	2.5 ± 0.6 (1.6–3.5)	0.5 ± 0.7 (0.1–2.0)	1.5 ± 0.4 (1.0–2.1)
CD62L	63.1 ± 11.1 (47.7–78.8)	57.9 ± 18.3 (32.4–77.0)	88.5 ± 15.4 (54.6–98.7)	81.9 ± 17.3 (55.7–93.9)
CCR7	74.1 ± 15.3 (43.1–93.3)	55.7 ± 15.7 (36.7–73.3)	1.0 ± 0.8 (0–2.4)	2.7 ± 2.4 (0.5–7.5)
CD2	99.5 ± 0.6 (98.7–100)	87.7 ± 9.3 (71.6–94.1)	1.1 ± 0.8 (0.3–2.2)	48.3 ± 10.0 (31.2–55.7)
CD27	85.9 ± 7.7 (75.2–94.3)	88.4 ± 8.0 (74.8–94.1)	0.7 ± 0.4 (0.2–1.2)	1.8 ± 0.6 (0.8–2.3)
CD28	99.1 ± 0.8 (97.8–100)	72.0 ± 7.3 (62.4–82.4)	85.4 ± 6.7 (78.9–95.3)	13.9 ± 8.1 (6.9–27.3)
CD45RO	68.0 ± 14.0 (44.6–92.4)	31.0 ± 16.7 (7.8–64.5)	5.6 ± 6.2 (1.3–28.1)	2.8 ± 2.7 (0.9–12.7)

The frequency (%) of surface markers on ILC subsets are expressed as the mean ± SD (range) for chemokine receptors and adhesion molecules ($n = 5-7$), costimulatory molecules ($n = 5$), and CD45RO ($n = 20$). Representative flow plots are shown in Fig. 4.

As with the chemokine receptors, we found substantial heterogeneity in the expression of costimulatory markers among the different peripheral blood ILC subsets (Fig. 4B, Table II). The majority of all ILC1 subsets expressed CD28, CD27, and CD2, costimulatory markers that are constitutively expressed on T cells (45–47). In contrast, ILC2 expressed CD28, but not CD27 or CD2, whereas a fraction of ILC3 expressed CD2 and CD28 but not CD27. Interestingly, we found that ILC1, but not ILC2 or ILC3, expressed CD45RO, a marker used to identify memory T lymphocyte subsets (Fig. 4B, Table II) (48). When we examined ILC subsets in cord blood, all ILC subsets were present and expressed similar patterns of CD28 compared with adult PBMC, yet CD45RO was low to absent in cord blood ILC (Supplemental Fig. 4).

These data suggest unique functions or migratory patterns for CD4⁺ ILC1 compared with other ILC1 populations, but the similarities in CCR7, costimulatory marker, and CD45RO expression in ILC1 suggest common modes of regulation among the ILC1 subsets.

CD4⁺ ILC1 coexpress IL-6R α and gp130 and respond to IL-6

To further examine factors that may differentially regulate the ILC subsets, we examined whether these subsets were responsive to IL-6, a cytokine that is thought to be important in autoimmune disease pathogenesis (49). Only CD4⁺ ILC1 had a high frequency of cells expressing both IL-6R α and gp130 (Fig. 5A, 5C). In some individuals, ILC2 also had substantial expression of IL-6R α , although the majority of IL-6R α ⁺ ILC2 did not coexpress gp130. Importantly, IL-6 responsiveness, as measured by STAT-3 and STAT-1 phosphorylation after IL-6 stimulation, paralleled the frequency of IL-6R α and gp130 coexpression on the various ILC subsets (Fig. 5B, 5C). Thus, compared with other ILC subsets, CD4⁺ ILC1 are uniquely IL-6 responsive.

A small set of genes distinguishes CD4⁺ and CD4⁻ ILC1 transcriptional profiles

Although CD4⁺ ILC1 exhibited substantial heterogeneity in surface marker expression, we were interested in determining whether there was a core transcriptional profile that distinguished CD4⁺ ILC1 from CD4⁻ ILC1. To address this question, we performed RNA sequencing (RNAseq) on peripheral blood CD4⁺ and CD4⁻ ILC1 isolated from three healthy control subjects. We found that a total of 66 genes was differentially expressed between CD4⁺ and CD4⁻ ILC1, with 50 genes that were upregulated and 16 that were downregulated in CD4⁺ ILC1 compared with CD4⁻

ILC1 (Fig. 6). A variety of cellular processes was represented by these differentially expressed genes; only a small number was immune-regulatory genes (50, 51). Of these immune-related genes, CD4, CD8 α , CD8 β , and CRTAM are also differentially expressed between CD4⁺ and CD8⁺ T lymphocytes (52). In addition, the IL-18R subunit IL18R1 and AICD genes were expressed more highly in CD4⁺ ILC1. Although the best characterized role for AICD is in B cell class switching, several reports also suggest that it is involved in innate antiviral immunity (53). These data indicate that a small set of genes does differentiate CD4⁺ from CD4⁻ ILC1.

Peripheral blood ILC subset frequencies are altered in SSc

To apply these phenotypic analyses to a systemic disease, we chose to examine ILC subset frequencies in SSc, an autoimmune disease in which vascular dysfunction and fibrosis of the skin and other organs lead to substantial morbidity and mortality (54). Although there is clearly immune dysregulation in SSc, the mechanisms involved in disease pathogenesis are poorly understood. Type 2 inflammatory cytokines, particularly IL-13, are thought to be central drivers of fibrosis in SSc, although Th17 and Th22 cells have also been implicated in SSc disease pathogenesis (55–58). When we compared ILC subset frequencies in PBMC from patients with SSc with those from age- and gender-matched control subjects, we were surprised to find that, although ILC2 frequencies were not significantly different, ILC1 and NKp44⁺ ILC3 frequencies were increased and NKp44⁻ ILC3 frequencies were decreased in SSc relative to the total peripheral blood ILC (Lin⁻CD127⁺) population and total live CD45⁺ lymphocytes (Fig. 7A). Analyses of some of the subjects shown in Fig. 7A included staining for CD4. In this cohort, we found that the enrichment of ILC1 in SSc was primarily attributable to changes in CD4⁺ ILC (Fig. 7B). These data examining CD4⁺ and CD4⁻ ILC1 were confirmed in a second age- and gender-matched cohort, which demonstrated increased frequencies in CD4⁺ and CD4⁻ ILC1 in SSc within the total ILC population but significant increases only in CD4⁺ ILC1 within total live CD45⁺ lymphocytes (Fig. 7B). Expression patterns of the costimulatory markers CD2, CD27, and CD28 in ILC subsets from SSc were similar to those seen in controls (Fig. 7C).

Because IL-6 signaling has been implicated in inflammation and fibrosis in SSc (56, 59–61), we also investigated IL-6R α expression on ILC subsets in the peripheral blood of SSc patients compared with age- and gender-matched controls. Interestingly, we found a decrease in the percentage of CD4⁺ ILC1 coexpressing

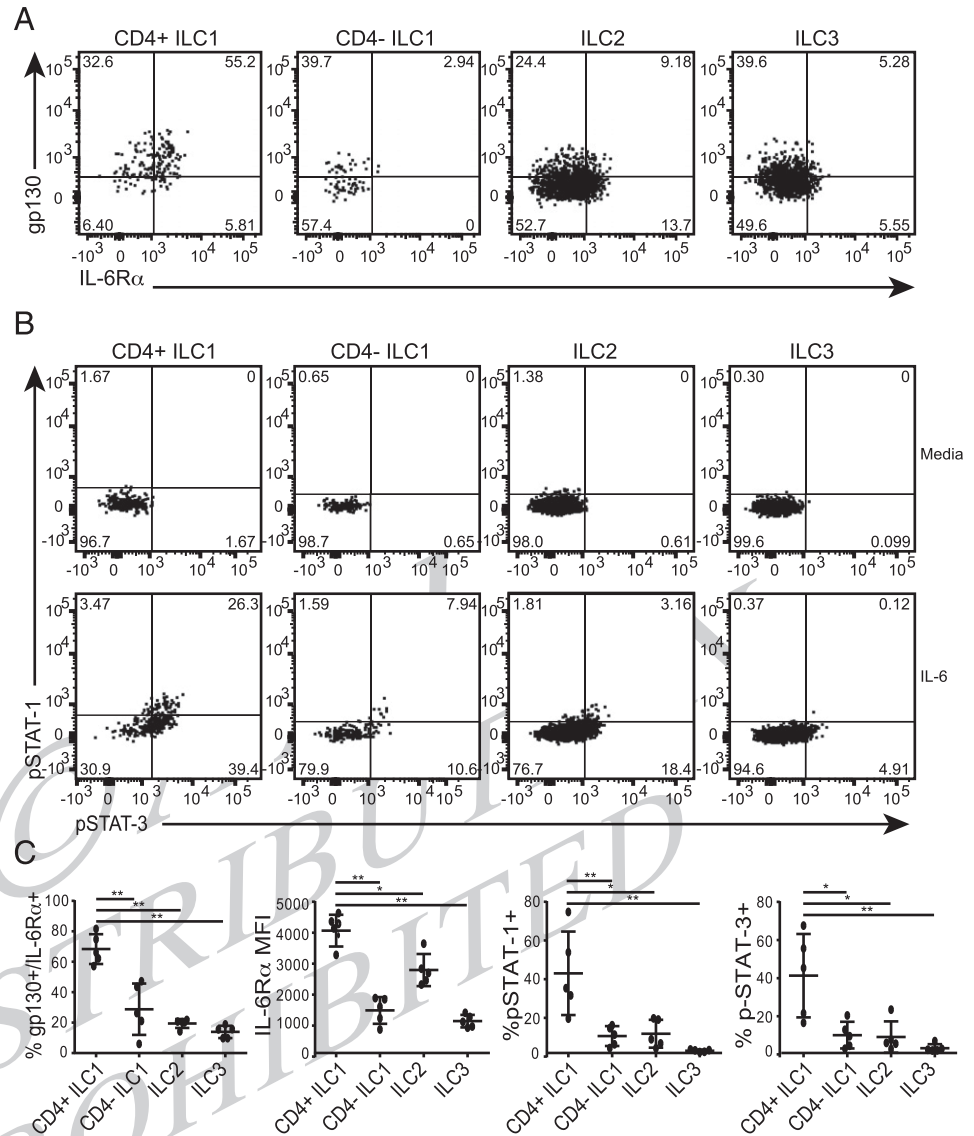


FIGURE 5. High frequency of IL-6R α expression on CD4⁺ ILC1. Fresh or frozen PBMC were analyzed for IL-6R α and gp130 expression on ILC subsets (**A**) and phosphorylation of STAT-1 and STAT-3 following a 20-min stimulation with 5 ng/ml of IL-6 (**B**). Flow plots are representative stains from $n > 5$ subjects for each stain set. (**C**) gp130⁺/IL-6R α ⁺ frequencies, IL-6R α MFI, and post-stimulation p-STAT-1 and p-STAT-3 frequencies in ILC subsets from fresh PBMC ($n = 5$ /stain set). * $p < 0.05$, ** $p < 0.01$, two-tailed unpaired Mann-Whitney test.

IL-6R α and gp130 in SSc and a decrease in IL-6R α mean fluorescence intensity (MFI) on CD4⁺ ILC1 in SSc compared with controls (Fig. 7D).

Discussion

Through a comprehensive evaluation of chemokine receptors, adhesion molecules, costimulatory markers, and cytokines expressed by human peripheral blood ILC, we characterized distinct patterns within the ILC subsets that may further delineate their migration and function. Of particular note, we discovered a previously unappreciated heterogeneity in the ILC1 subset, which included CD4⁺, CD8⁺, and DN populations. We were surprised to find that CD4⁺ and CD4⁻ ILC1, but not ILC2 or ILC3, expressed significant levels of intracellular CD3 ϵ , suggesting a developmental relationship among the ILC1 populations that may be distinct from ILC2 and ILC3. Previous work demonstrated that NKp44⁻ ILC3 have the capacity to differentiate into NKp44⁺ ILC3 or ILC1 in vitro, depending on the cytokine milieu (30). Whether the ILC1 subsets that we describe are distinct from those that differentiate from ILC3 remains unclear.

Some NK cells also express intracellular CD3 components (62–64); however, the cell subsets in our analyses are distinct from classic NK cells based on a lack of CD16, CD56, perforin, and

granzyme B expression (29). Unlike CD4⁺ ILC1, CD8⁺ ILC1 had high frequencies of Eomes and T-bet coexpression, suggesting that they may share significant phenotypic and functional characteristics with NK cells. In contrast to CD8⁺ and DN ILC1, which displayed prominent Th1-like phenotypes, a substantial percentage of CD4⁺ cells lacked CXCR3, T-bet, and IFN- γ expression. Interestingly, CD4⁺ ILC1 were more potent producers of TNF- α , GM-CSF, and IL-2 and also included populations expressing CCR4, CCR10, and CXCR5. Given these phenotypic and functional differences between CD4⁺ and CD4⁻ ILC1, CD4⁺ ILC1 may represent a distinct subset, whereas DN and CD8⁺ ILC1 are likely more related to one another. A re-examination of these different ILC1 populations that incorporates functional analyses beyond the Th1 paradigm may better define conditions in which ILC1 are simply a source of IFN- γ , as well as when they may modulate inflammatory responses through other pathways.

Comparisons of ILC1 with ILC2 and ILC3 also highlighted other phenotypic features that were distinct among these populations. Only the ILC1 subsets express the T cell memory marker CD45RO. In addition, a large percentage of CD4⁺ and CD4⁻ ILC1 coexpressed CD62L and CCR7, which was absent on ILC2 and ILC3. In this manner, the ILC1 subsets closely resemble central memory T lymphocytes in phenotype (65). CCR7 is involved in the traf-

863
864
865
866
867
868
869
870
871
872
873
874
875
876
877
878
879
880
881
882
883
884
885
886
887
888
889
890
891
892
893
894
895
896
897
898
899
900
901
902
903
904
905
906
907
908
909
910
911
912
913
914
915
916
917
918
919
920
921
922
923
924
925
926
927
928
929
930
931
932
933
934
935
936
937
938
939
940
941
942
943
944
945
946
947
948
949
950
951
952
953
954
955
956
957
958
959
960
961
962
963
964
965
966
967
968
969
970
971
972
973
974
975
976
977
978
979
980
981
982
983
984
985
986
987
988
989
990

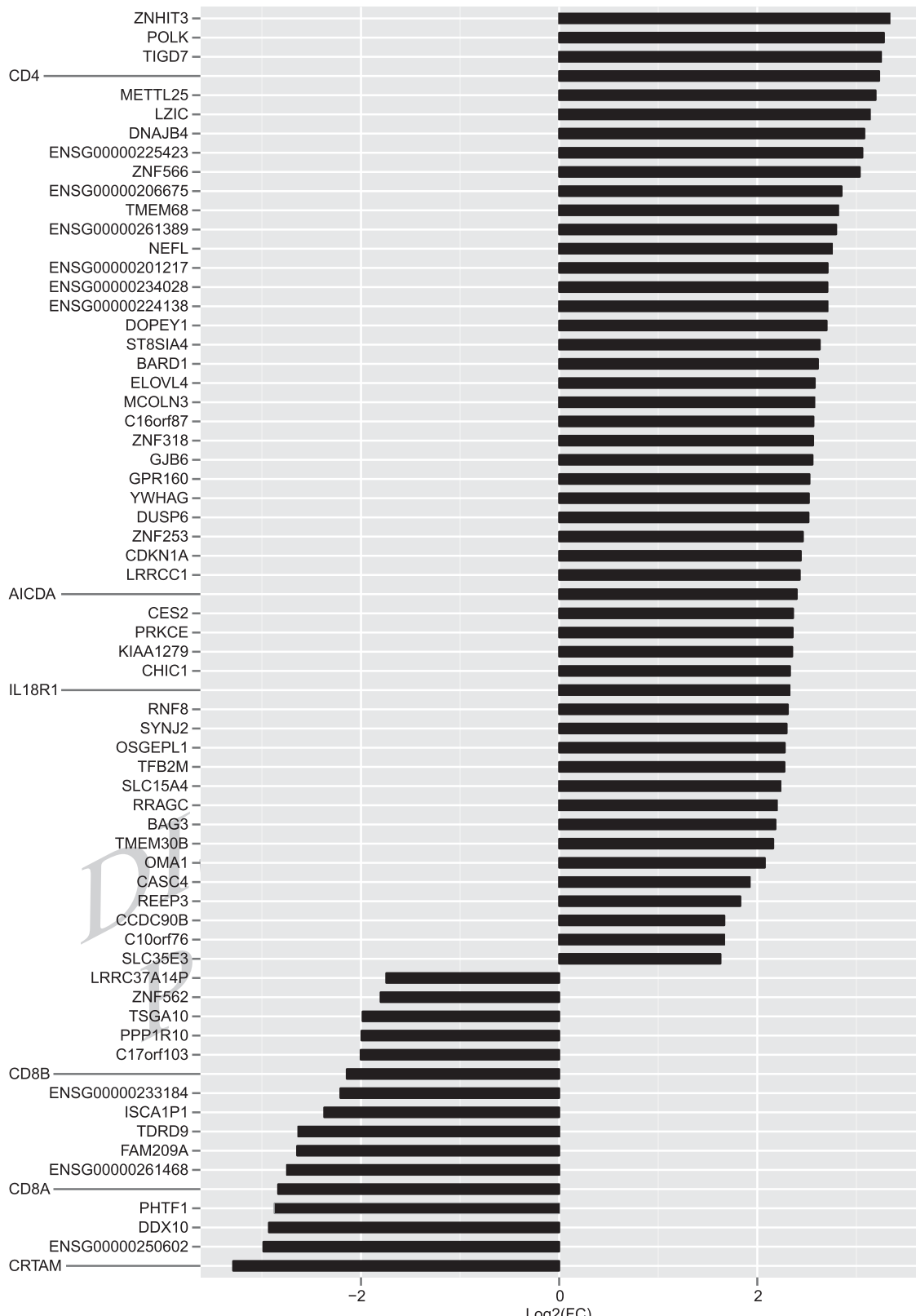


FIGURE 6. A small number of genes are differentially expressed in CD4⁺ versus CD4⁻ ILC1. RNAseq was performed on peripheral blood CD4⁺ and CD4⁻ ILC1 from three healthy control subjects. The fold change, expressed as Log2(FC), of genes with a false-discovery rate < 0.05 using DESeq2 was considered significant.

ficking of certain T cell subsets to secondary lymphoid organs; the expression of the CCR7 ligands CCL19 and CCL21 on non-hematopoietic cells in the lymph node allows colocalization of CCR7⁺ T cells and activated dendritic cells to more efficiently initiate an immune response (66, 67). Although other ILC subsets

are also present in lymphoid organs, such as the tonsils (68), CCR7 expression on ILC1 may suggest that this population is more actively recruited to lymphoid organs, or preferentially localized to lymph node T cell areas, where they may be more intimately associated with activated dendritic cells and T cells.

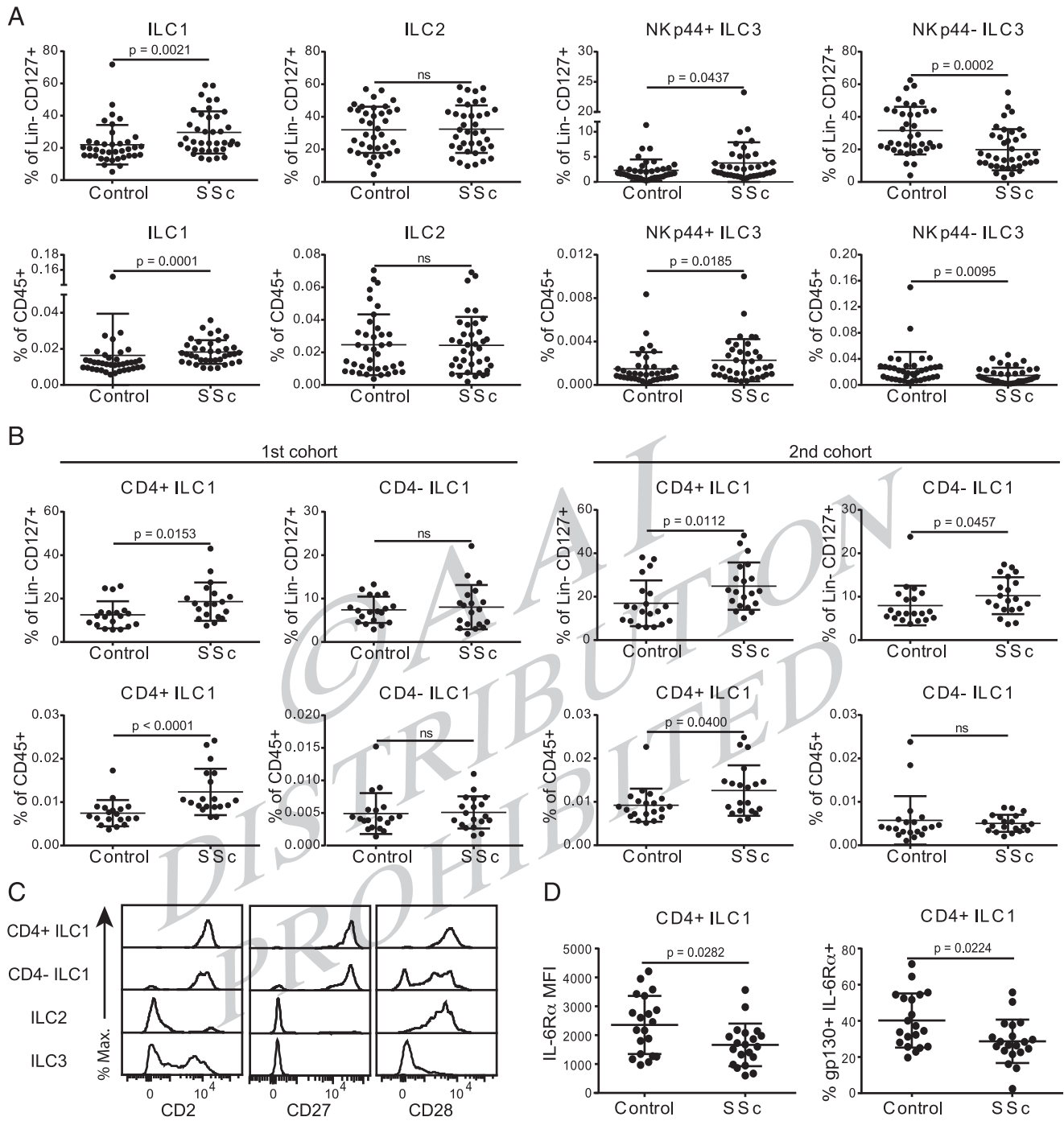


FIGURE 7. Altered ILC subset frequencies in SSc. **(A)** Frozen PBMC from gender- and age-matched controls and SSc subjects were thawed, stained for ILC subsets, and then analyzed by flow cytometry using the gating strategy outlined in Fig. 1A ($n = 38$ /cohort). **(B)** A subgroup of the subjects examined in (A) designated “1st cohort,” included analyses of CD4 expression, and these data on CD4⁺ and CD4⁻ ILC1 frequencies were replicated in a second cohort of age- and gender-matched control and SSc subjects ($n = 19 - 20$ per cohort). **(C)** ILC subset expression of CD2, CD27 and CD28 was examined on previously frozen PBMC from SSc subjects. Histograms are representative staining from $n = 5$ subjects. **(D)** ILC subset expression of IL-6R α and gp130 was examined on previously frozen PBMC samples from control and SSc subjects ($n = 20$ /cohort). The p values were determined using two-tailed unpaired Mann-Whitney tests.

Recently, a distinct subset of memory CD4⁺ T lymphocytes was described that migrates from the skin to draining lymph nodes in a CCR7-dependent manner and then re-enters the peripheral circulation, which allows this subset to provide help to distal lymphoid and cutaneous tissues (69). It is interesting to speculate that a similar scenario may exist for ILC1. Distinct patterns of expression of the costimulatory markers CD2, CD27, and CD28 also suggest that ILC1 may differ from ILC2 and ILC3 in how they are activated, as well as in the cell types with which they interact.

An examination of peripheral blood ILC in SSc, a disease with prominent fibrotic features, revealed that ILC1 and NKp44⁺ ILC3 were increased in frequency, whereas NKp44⁻ ILC3 were decreased in subjects with SSc. Additionally, the increase in ILC1 frequencies was primarily attributable to changes in CD4⁺ ILC1, which express lower levels of T-bet and IFN- γ than CD4⁻ ILC1. This is of particular interest because T-bet-deficient mice display increased sensitivity to the bleomycin-induced dermal sclerosis model of SSc in a T cell-independent manner (70). In light of

numerous studies in mouse models and in humans that implicate TNF- α and GM-CSF in the pathogenesis of several autoimmune diseases (71, 72), it is also intriguing that multiple ILC subsets can produce these cytokines and that CD4⁺ ILC1 appear to be more potent producers of TNF- α and GM-CSF than are CD4⁻ ILC1.

CD4⁺ ILC1 were also the most responsive to IL-6, another cytokine that is thought to play an important role in autoimmunity (49). IL-6 and soluble IL-6R α were reported to be elevated in SSc (56, 59, 61, 73, 74). However, we were surprised to find that the frequencies of CD4⁺ ILC1 expressing IL-6R α were decreased in SSc. Although these data suggest that increased IL-6 signaling in CD4⁺ ILC1 may not be critical to SSc pathogenesis, CD4⁺ ILC1, as well as ILC2, which can also express significant levels of IL-6R α , may serve as sources of soluble IL-6R α , which can amplify IL-6 responses in inflammatory conditions (75). IL-6R α was shown to be downregulated upon T cell stimulation; thus, decreased IL-6R α expression on ILC in SSc could also result from increased ILC activation during disease (76).

Because SSc is a very heterogeneous disease that may involve distinct pathogenic mechanisms in early versus late disease, it will be important to understand how ILC frequencies change in different stages and subsets of disease. We defined important phenotypic and functional features of ILC subsets in the peripheral blood. More in-depth analyses of how the ILC populations that we describe may differ from those in tissue will better define their roles in autoimmune disease pathogenesis and help to establish whether ILC2 are functionally different in SSc.

Currently, tocilizumab, an anti-IL-6R mAb, and abatacept (CTLA4-Ig), which blocks interactions between CD28 and CD80 or CD86, have shown promise in small studies (77–79), and both are in clinical trials for SSc. The differential expression of IL-6R α and CD28 on ILC subsets suggests that not all ILC will be affected by these biologics to the same degree. Dysregulation of the innate immune compartment may be an important process that underlies the development of autoimmunity; thus, the ability of these therapies to appropriately target innate cells, such as ILC, is likely to have an important impact on therapeutic efficacy. Evaluation of how ILC subsets change during therapy, as well as whether changes in these subsets correlate with clinical response, will give insight into the mechanisms of disease and therapeutic efficacy and may aid the design of the next generation of biologics.

Acknowledgments

We thank Thien-Son Nguyen and all members of the BRI clinical core who aided in subject recruitment and samples management; Vivian Gersuk and the BRI genomics and bioinformatics core staff who performed the library construction, sequencing, and data processing for the RNAseq; and Alyssa Sheih for critical review of the manuscript.

Disclosures

The authors have no financial conflicts of interest.

References

- Nussbaum, J. C., S. J. Van Dyken, J. von Moltke, L. E. Cheng, A. Mohapatra, A. B. Molofsky, E. E. Thornton, M. F. Krummel, A. Chawla, H.-E. Liang, and R. M. Locksley. 2013. Type 2 innate lymphoid cells control eosinophil homeostasis. *Nature* 502: 245–248.
- Lee, M.-W., J. I. Odegaard, L. Mukundan, Y. Qiu, A. B. Molofsky, J. C. Nussbaum, K. Yun, R. M. Locksley, and A. Chawla. 2015. Activated type 2 innate lymphoid cells regulate beige fat biogenesis. *Cell* 160: 74–87.
- Brestoff, J. R., B. S. Kim, S. A. Saenz, R. R. Stine, L. A. Monticelli, G. F. Sonnenberg, J. J. Thome, D. L. Farber, K. Lutfy, P. Seale, and D. Artis. 2015. Group 2 innate lymphoid cells promote beiging of white adipose tissue and limit obesity. *Nature* 519: 242–246.
- Van Gool, F., A. B. Molofsky, M. M. Morar, M. Rosenzweig, H.-E. Liang, D. Klatzmann, R. M. Locksley, and J. A. Bluestone. 2014. Interleukin-5-

- producing group 2 innate lymphoid cells control eosinophilia induced by interleukin-2 therapy. *Blood* 124: 3572–3576.
- Sawa, S., M. Lochner, N. Satoh-Takayama, S. Dulauroy, M. Béard, M. Kleinschek, D. Cua, J. P. Di Santo, and G. Eberl. 2011. ROR γ ⁺ innate lymphoid cells regulate intestinal homeostasis by integrating negative signals from the symbiotic microbiota. *Nat. Immunol.* 12: 320–326.
- Goto, Y., T. Obata, J. Kunisawa, S. Sato, I. I. Ivanov, A. Lamichhane, N. Takeyama, M. Kamioka, M. Sakamoto, T. Matsuki, et al. 2014. Innate lymphoid cells regulate intestinal epithelial cell glycosylation. *Science* 345: 1254009.
- Hepworth, M. R., L. A. Monticelli, T. C. Fung, C. G. K. Ziegler, S. Grunberg, R. Sinha, A. R. Mantegazza, H.-L. Ma, A. Crawford, J. M. Angelosanto, et al. 2013. Innate lymphoid cells regulate CD4⁺ T-cell responses to intestinal commensal bacteria. *Nature* 498: 113–117.
- Mirchandani, A. S., A.-G. Besnard, E. Yip, C. Scott, C. C. Bain, V. Cerovic, R. J. Salmond, and F. Y. Liew. 2014. Type 2 innate lymphoid cells drive CD4⁺ Th2 cell responses. *J. Immunol.* 192: 2442–2448.
- Oliphant, C. J., Y. Y. Hwang, J. A. Walker, M. Salimi, S. H. Wong, J. M. Brewer, A. Englezakis, J. L. Barlow, E. Hams, S. T. Scanlon, et al. 2014. MHCII-mediated dialog between group 2 innate lymphoid cells and CD4⁺ T cells potentiates type 2 immunity and promotes parasitic helminth expulsion. *Immunity* 41: 283–295.
- von Burg, N., S. Chappaz, A. Baerenwaldt, E. Horvath, S. Bose Dasgupta, D. Ashok, J. Pieters, F. Tacchini-Cottier, A. Rolink, H. Acha-Orbea, and D. Finke. 2014. Activated group 3 innate lymphoid cells promote T-cell-mediated immune responses. *Proc. Natl. Acad. Sci. USA* 111: 12835–12840.
- Klose, C. S., E. A. Kiss, V. Schwierzeck, K. Ebert, T. Hoyler, Y. d'Hargues, N. Göppert, A. L. Croxford, A. Waisman, Y. Tanriver, and A. Diefenbach. 2013. A T-bet gradient controls the fate and function of CCR6-ROR γ ⁺ innate lymphoid cells. *Nature* 494: 261–265.
- Klose, C. S., M. Flach, L. Möhle, L. Rogell, T. Hoyler, K. Ebert, C. Fabiunke, D. Pfeifer, V. Sexl, D. Fonseca-Pereira, et al. 2014. Differentiation of type 1 ILCs from a common progenitor to all helper-like innate lymphoid cell lineages. *Cell* 157: 340–356.
- Neill, D. R., S. H. Wong, A. Bellosi, R. J. Flynn, M. Daly, T. K. Langford, C. Bucks, C. M. Kane, P. G. Fallon, R. Pannell, et al. 2010. Nuocytes represent a new innate effector leukocyte that mediates type-2 immunity. *Nature* 464: 1367–1370.
- Monticelli, L. A., G. F. Sonnenberg, M. C. Abt, T. Alenghat, C. G. Ziegler, T. A. Doering, J. M. Angelosanto, B. J. Laidlaw, C. Y. Yang, T. Sathaliyawala, et al. 2011. Innate lymphoid cells promote lung-tissue homeostasis after infection with influenza virus. *Nat. Immunol.* 12: 1045–1054.
- Halim, T. Y., R. H. Krauss, A. C. Sun, and F. Takei. 2012. Lung natural helper cells are a critical source of Th2 cell-type cytokines in protease allergen-induced airway inflammation. *Immunity* 36: 451–463.
- Klein Wolterink, R. G., A. Kleijnjan, M. van Nimwegen, I. Bergen, M. de Bruijn, Y. Levani, and R. W. Hendriks. 2012. Pulmonary innate lymphoid cells are major producers of IL-5 and IL-13 in murine models of allergic asthma. *Eur. J. Immunol.* 42: 1106–1116.
- Buonocore, S., P. P. Ahern, H. H. Uhlig, I. I. Ivanov, D. R. Littman, K. J. Maloy, and F. Powrie. 2010. Innate lymphoid cells drive interleukin-23-dependent innate intestinal pathology. *Nature* 464: 1371–1375.
- Sonnenberg, G. F., L. A. Monticelli, M. M. Elloso, L. A. Fouser, and D. Artis. 2011. CD4⁺ lymphoid tissue-inducer cells promote innate immunity in the gut. *Immunity* 34: 122–134.
- Perry, J. S., S. Han, Q. Xu, M. L. Herman, L. B. Kennedy, G. Csako, and B. Bielekova. 2012. Inhibition of LTI cell development by CD25 blockade is associated with decreased intrathecal inflammation in multiple sclerosis. *Sci. Transl. Med.* 4: 145ra106.
- Dyring-Andersen, B., C. Geisler, C. Agerbeck, J. P. Lauritsen, S. D. Gúdjonsdóttir, L. Skov, and C. M. Bonefeld. 2014. Increased number and frequency of group 3 innate lymphoid cells in nonlesional psoriatic skin. *Br. J. Dermatol.* 170: 609–616.
- Teunissen, M. B., J. M. Munneke, J. H. Bernink, P. I. Spuls, P. C. Res, A. Te Velde, S. Cheuk, M. W. Brouwer, S. P. Menting, L. Eidsmo, et al. 2014. Composition of innate lymphoid cell subsets in the human skin: enrichment of NCR (+) ILC3 in lesional skin and blood of psoriasis patients. *J. Invest. Dermatol.* 134: 2351–2360.
- Geremia, A., C. V. Arancibia-Carcamo, M. P. Fleming, N. Rust, B. Singh, N. J. Mortensen, S. P. L. Travis, and F. Powrie. 2011. IL-23-responsive innate lymphoid cells are increased in inflammatory bowel disease. *J. Exp. Med.* 208: 1127–1133.
- Mjösberg, J. M., S. Trifari, N. K. Crellin, C. P. Peters, C. M. van Drunen, B. Piet, W. J. Fokkens, T. Cupedo, and H. Spits. 2011. Human IL-25- and IL-33-responsive type 2 innate lymphoid cells are defined by expression of CRTH2 and CD161. *Nat. Immunol.* 12: 1055–1062.
- Kim, B. S., M. C. Siracusa, S. A. Saenz, M. Noti, L. A. Monticelli, G. F. Sonnenberg, M. R. Hepworth, A. S. Van Voorhees, M. R. Comeau, and D. Artis. 2013. TSLP elicits IL-33-independent innate lymphoid cell responses to promote skin inflammation. *Sci. Transl. Med.* 5: 170ra16.
- Bartemes, K. R., G. M. Kephart, S. J. Fox, and H. Kita. 2014. Enhanced innate type 2 immune response in peripheral blood from patients with asthma. *J. Allergy Clin. Immunol.* 134: 671–678.e4.
- Barnig, C., M. Cernadas, S. Dutile, X. Liu, M. A. Perrella, S. Kazani, M. E. Wechsler, E. Israel, and B. D. Levy. 2013. Lipoxin A4 regulates natural killer cell and type 2 innate lymphoid cell activation in asthma. *Sci. Transl. Med.* 5: 174ra26.
- Villanova, F., B. Flutter, I. Tosi, K. Grys, H. Sreeneebus, G. K. Perera, A. Chapman, C. H. Smith, P. Di Meglio, and F. O. Nestle. 2014. Characterization

1247
1248
1249
1250
1251
1252
1253
1254
1255
1256
1257
1258
1259
1260
1261
1262
1263
1264
1265
1266
1267
1268
1269
1270
1271
1272
1273
1274
1275
1276
1277
1278
1279
1280
1281
1282
1283
1284
1285
1286
1287
1288
1289
1290
1291
1292
1293
1294
1295
1296
1297
1298
1299
1300
1301
1302
1303
1304
1305
1306
1307
1308
1309
1310

1311
1312
1313
1314
1315
1316
1317
1318
1319
1320
1321
1322
1323
1324
1325
1326
1327
1328
1329
1330
1331
1332
1333
1334
1335
1336
1337
1338
1339
1340
1341
1342
1343
1344
1345
1346
1347
1348
1349
1350
1351
1352
1353
1354
1355
1356
1357
1358
1359
1360
1361
1362
1363
1364
1365
1366
1367
1368
1369
1370
1371
1372
1373
1374

- of innate lymphoid cells in human skin and blood demonstrates increase of Nkp44+ ILC3 in psoriasis. *J. Invest. Dermatol.* 134: 984–991.
28. Spits, H., D. Artis, M. Colonna, A. Dieffenbach, J. P. Di Santo, G. Eberl, S. Koyasu, R. M. Locksley, A. N. J. McKenzie, R. E. Mebius, et al. 2013. Innate lymphoid cells—a proposal for uniform nomenclature. *Nat. Rev. Immunol.* 13: 145–149.
 29. Huntington, N. D., C. A. Vosshenrich, and J. P. Di Santo. 2007. Developmental pathways that generate natural-killer-cell diversity in mice and humans. *Nat. Rev. Immunol.* 7: 703–714.
 30. Bernink, J. H., C. P. Peters, M. Munneke, A. A. te Velde, S. L. Meijer, K. Weijer, H. S. Hreggvidsdottir, S. E. Heinsbroek, N. Legrand, C. J. Buskens, et al. 2013. Human type 1 innate lymphoid cells accumulate in inflamed mucosal tissues. *Nat. Immunol.* 14: 221–229.
 31. Bekiaris, V., J. R. Sedy, M. Rossetti, R. Spreafico, S. Sharma, A. Rhode-Kurnow, B. C. Ware, N. Huang, M. G. Macaulay, P. S. Norris, et al. 2013. Human CD4 +CD3– innate-like T cells provide a source of TNF and lymphotoxin- $\alpha\beta$ and are elevated in rheumatoid arthritis. *J. Immunol.* 191: 4611–4618.
 32. Lazarevic, V., L. H. Glimcher, and G. M. Lord. 2013. T-bet: a bridge between innate and adaptive immunity. *Nat. Rev. Immunol.* 13: 777–789.
 33. Knox, J. J., G. L. Cosma, M. R. Betts, and L. M. McLane. 2014. Characterization of T-bet and comes in peripheral human immune cells. *Front. Immunol.* 5: 217.
 34. Yang, Y., J. Xu, Y. Niu, J. S. Bromberg, and Y. Ding. 2008. T-bet and eomesodermin play critical roles in directing T cell differentiation to Th1 versus Th17. *J. Immunol.* 181: 8700–8710.
 35. Pearce, E. L., A. C. Mullen, G. A. Martins, C. M. Krawczyk, A. S. Hutchins, V. P. Zediak, M. Banica, C. B. DiCiccio, D. A. Gross, C. A. Mao, et al. 2003. Control of effector CD8+ T cell function by the transcription factor Eomesodermin. *Science* 302: 1041–1043.
 36. Qin, S., J. B. Rottman, P. Myers, N. Kassam, M. Weinblatt, M. Loetscher, A. E. Koch, B. Moser, and C. R. Mackay. 1998. The chemokine receptors CXCR3 and CCR5 mark subsets of T cells associated with certain inflammatory reactions. *J. Clin. Invest.* 101: 746–754.
 37. Sallusto, F., D. Lenig, C. R. Mackay, and A. Lanzavecchia. 1998. Flexible programs of chemokine receptor expression on human polarized T helper 1 and 2 lymphocytes. *J. Exp. Med.* 187: 875–883.
 38. Acosta-Rodriguez, E. V., L. Rivino, J. Geginat, D. Jarrossay, M. Gattorno, A. Lanzavecchia, F. Sallusto, and G. Napolitano. 2007. Surface phenotype and antigenic specificity of human interleukin 17-producing T helper memory cells. *Nat. Immunol.* 8: 639–646.
 39. Singh, S. P., H. H. Zhang, J. F. Foley, M. N. Hedrick, and J. M. Farber. 2008. Human T cells that are able to produce IL-17 express the chemokine receptor CCR6. *J. Immunol.* 180: 214–221.
 40. Duhon, T., R. Geiger, D. Jarrossay, A. Lanzavecchia, and F. Sallusto. 2009. Production of interleukin 22 but not interleukin 17 by a subset of human skin-homing memory T cells. *Nat. Immunol.* 10: 857–863.
 41. Duhon, T., R. Duhon, A. Lanzavecchia, F. Sallusto, and D. J. Campbell. 2012. Functionally distinct subsets of human FOXP3+ Treg cells that phenotypically mirror effector Th cells. *Blood* 119: 4430–4440.
 42. Trifari, S., C. D. Kaplan, E. H. Tran, N. K. Crellin, and H. Spits. 2009. Identification of a human helper T cell population that has abundant production of interleukin 22 and is distinct from T(H)-17, T(H)1 and T(H)2 cells. *Nat. Immunol.* 10: 864–871.
 43. Williams, I. R. 2004. Chemokine receptors and leukocyte trafficking in the mucosal immune system. *Immunol. Res.* 29: 283–292.
 44. Islam, S. A., and A. D. Luster. 2012. T cell homing to epithelial barriers in allergic disease. *Nat. Med.* 18: 705–715.
 45. Lenschow, D. J., T. L. Walunas, and J. A. Bluestone. 1996. CD28/B7 system of T cell costimulation. *Annu. Rev. Immunol.* 14: 233–258.
 46. van Lier, R. A., J. Borst, T. M. Vroom, H. Klein, P. Van Mourik, W. P. Zeijlemaker, and C. J. Melief. 1987. Tissue distribution and biochemical and functional properties of Tp55 (CD27), a novel T cell differentiation antigen. *J. Immunol.* 139: 1589–1596.
 47. Moingeon, P., H. C. Chang, P. H. Sayre, L. K. Clayton, A. Alcover, P. Gardner, and E. L. Reinherz. 1989. The structural biology of CD2. *Immunol. Rev.* 111: 111–144.
 48. Sallusto, F., J. Geginat, and A. Lanzavecchia. 2004. Central memory and effector memory T cell subsets: function, generation, and maintenance. *Annu. Rev. Immunol.* 22: 745–763.
 49. Tanaka, T., M. Narazaki, and T. Kishimoto. 2014. IL-6 in inflammation, immunity, and disease. *Cold Spring Harb. Perspect. Biol.* 6: a016295.
 50. Huang, W., B. T. Sherman, and R. A. Lempicki. 2009. Systematic and integrative analysis of large gene lists using DAVID bioinformatics resources. *Nat. Protoc.* 4: 44–57.
 51. Huang, W., B. T. Sherman, and R. A. Lempicki. 2009. Bioinformatics enrichment tools: paths toward the comprehensive functional analysis of large gene lists. *Nucleic Acids Res.* 37: 1–13.
 52. Abbas, A. R., D. Baldwin, Y. Ma, W. Ouyang, A. Gurney, F. Martin, S. Fong, M. van Lookeren Campagne, P. Godowski, P. M. Williams, et al. 2005. Immune response in silico (IRIS): immune-specific genes identified from a compendium of microarray expression data. *Genes Immun.* 6: 319–331.
 53. Moris, A., S. Murray, and S. Cardinaud. 2014. AID and APOBECs span the gap between innate and adaptive immunity. *Front. Microbiol.* 5: 534.
 54. Gabrielli, A., E. V. Avvedimento, and T. Krieg. 2009. Scleroderma. *N. Engl. J. Med.* 360: 1989–2003.
 55. Barron, L., and T. A. Wynn. 2011. Fibrosis is regulated by Th2 and Th17 responses and by dynamic interactions between fibroblasts and macrophages. *Am. J. Physiol. Gastrointest. Liver Physiol.* 300: G723–G728.
 56. Radstake, T. R., L. van Bon, J. Broen, A. Hussiani, R. Hesselstrand, D. M. Wuttge, Y. Deng, R. Simms, E. Lubberts, and R. Lafyatis. 2009. The pronounced Th17 profile in systemic sclerosis (SSc) together with intracellular expression of TGFbeta and IFNgamma distinguishes SSc phenotypes. *PLoS One* 4: e5903.
 57. Truchetet, M.-E., N. C. Brembilla, E. Montanari, Y. Allanore, and C. Chizzolini. 2011. Increased frequency of circulating Th22 in addition to Th17 and Th2 lymphocytes in systemic sclerosis: association with interstitial lung disease. *Arthritis Res. Ther.* 13: R166.
 58. Mathian, A., C. Parizot, K. Dorgham, S. Trad, L. Arnaud, M. Larsen, M. Miyara, M. Hié, J.-C. Piette, C. Frances, et al. 2012. Activated and resting regulatory T cell exhaustion concurs with high levels of interleukin-22 expression in systemic sclerosis lesions. *Ann. Rheum. Dis.* 71: 1227–1234.
 59. Hasegawa, M., S. Sato, M. Fujimoto, H. Ihn, K. Kikuchi, and K. Takehara. 1998. Serum levels of interleukin 6 (IL-6), oncostatin M, soluble IL-6 receptor, and soluble gp130 in patients with systemic sclerosis. *J. Rheumatol.* 25: 308–313.
 60. De Laetis, A., P. Sestini, P. Pantelidis, R. Hoyles, D. M. Hansell, N. S. Goh, C. J. Zappala, D. Visca, T. M. Maher, C. P. Denton, et al. 2013. Serum interleukin 6 is predictive of early functional decline and mortality in interstitial lung disease associated with systemic sclerosis. *J. Rheumatol.* 40: 435–446.
 61. Needleman, B. W., F. M. Wigley, and R. W. Stair. 1992. Interleukin-1, interleukin-2, interleukin-4, interleukin-6, tumor necrosis factor alpha, and interferon-gamma levels in sera from patients with scleroderma. *Arthritis Rheum.* 35: 67–72.
 62. Phillips, J. H., T. Hori, A. Nagler, N. Bhat, H. Spits, and L. L. Lanier. 1992. Ontogeny of human natural killer (NK) cells: fetal NK cells mediate cytolytic function and express cytoplasmic CD3 epsilon,delta proteins. *J. Exp. Med.* 175: 1055–1066.
 63. Lanier, L. L., C. Chang, H. Spits, and J. H. Phillips. 1992. Expression of cytoplasmic CD3 epsilon proteins in activated human adult natural killer (NK) cells and CD3 gamma, delta, epsilon complexes in fetal NK cells. Implications for the relationship of NK and T lymphocytes. *J. Immunol.* 149: 1876–1880.
 64. Biassoni, R., S. Ferrini, I. Prigione, A. Moretta, and E. O. Long. 1988. CD3-negative lymphokine-activated cytotoxic cells express the CD3 epsilon gene. *J. Immunol.* 140: 1685–1689.
 65. Mueller, S. N., T. Gebhardt, F. R. Carbone, and W. R. Heath. 2013. Memory T cell subsets, migration patterns, and tissue residence. *Annu. Rev. Immunol.* 31: 137–161.
 66. Förster, R., A. Schubel, D. Breitfeld, E. Kremmer, I. Renner-Müller, E. Wolf, and M. Lipp. 1999. CCR7 coordinates the primary immune response by establishing functional microenvironments in secondary lymphoid organs. *Cell* 99: 23–33.
 67. Gunn, M. D., S. Kyuwa, C. Tam, T. Kakiuchi, A. Matsuzawa, L. T. Williams, and H. Nakano. 1999. Mice lacking expression of secondary lymphoid organ chemokine have defects in lymphocyte homing and dendritic cell localization. *J. Exp. Med.* 189: 451–460.
 68. Crellin, N. K., S. Trifari, C. D. Kaplan, T. Cupedo, and H. Spits. 2010. Human Nkp44+IL-22+ cells and LTI-like cells constitute a stable RORC+ lineage distinct from conventional natural killer cells. *J. Exp. Med.* 207: 281–290.
 69. Bromley, S. K., S. Yan, M. Tomura, O. Kanagawa, and A. D. Luster. 2013. Recirculating memory T cells are a unique subset of CD4+ T cells with a distinct phenotype and migratory pattern. *J. Immunol.* 190: 970–976.
 70. Aliprantis, A. O., J. Wang, J. W. Fathman, R. Lemaire, D. M. Dorfman, R. Lafyatis, and L. H. Glimcher. 2007. Transcription factor T-bet regulates skin sclerosis through its function in innate immunity and via IL-13. *Proc. Natl. Acad. Sci. USA* 104: 2827–2830.
 71. Croft, M., C. A. Benedict, and C. F. Ware. 2013. Clinical targeting of the TNF and TNFR superfamilies. *Nat. Rev. Drug Discov.* 12: 147–168.
 72. van Nieuwenhuijze, A., M. Koenders, D. Roelvelde, M. A. Sleeman, W. van den Berg, and I. P. Wicks. 2013. GM-CSF as a therapeutic target in inflammatory diseases. *Mol. Immunol.* 56: 675–682.
 73. Sato, S., M. Hasegawa, and K. Takehara. 2001. Serum levels of interleukin-6 and interleukin-10 correlate with total skin thickness score in patients with systemic sclerosis. *J. Dermatol. Sci.* 27: 140–146.
 74. Khan, K., S. Xu, S. Nihtyanova, E. Derrett-Smith, D. Abraham, C. P. Denton, and V. H. Ong. 2012. Clinical and pathological significance of interleukin 6 overexpression in systemic sclerosis. *Ann. Rheum. Dis.* 71: 1235–1242.
 75. Rose-John, S. 2012. IL-6 trans-signaling via the soluble IL-6 receptor: importance for the pro-inflammatory activities of IL-6. *Int. J. Biol. Sci.* 8: 1237–1247.
 76. Jones, G. W., R. M. McLoughlin, V. J. Hammond, C. R. Parker, J. D. Williams, R. Malhotra, J. Scheller, A. S. Williams, S. Rose-John, N. Topley, and S. A. Jones. 2010. Loss of CD4+ T cell IL-6R expression during inflammation underlines a role for IL-6 trans signaling in the local maintenance of Th17 cells. *J. Immunol.* 184: 2130–2139.
 77. Elhai, M., M. Meunier, M. Matucci-Cerinic, B. Maurer, G. Riemekasten, T. Leturcq, R. Pellerito, C. A. Von Mühlen, A. Vacca, P. Airo, et al; EUSTAR (EULAR Scleroderma Trials and Research group). 2013. Outcomes of patients with systemic sclerosis-associated polyarthritis and myopathy treated with tocilizumab or abatacept: a EUSTAR observational study. *Ann. Rheum. Dis.* 72: 1217–1220.
 78. Chakravarty, E. F., DFlorentino, MBennett, and L. Chung. 2011. A Pilot Study of Abatacept for the Treatment of Patients with Diffuse Cutaneous Systemic Sclerosis. *Arthritis Rheum.* 63 (Abstract Suppl.): 707.
 79. de Paoli, F. V., B. D. Nielsen, F. Rasmussen, B. Deleuran, and K. Søndergaard. 2014. Abatacept induces clinical improvement in patients with severe systemic sclerosis. *Scand. J. Rheumatol.* 43: 342–345.

AUTHOR QUERIES

AUTHOR PLEASE ANSWER ALL QUERIES

- 1—Please verify that the title, footnotes, author names, and affiliations are correct as set.
 - 2—If you provided an ORCID number at submission, please confirm that it appears correctly in the footnote on the opening page of this article.
 - 3—If possible, please list a department or division for the first affiliation.
 - 4—Please indicate the correct surname (family name) of each author for indexing purposes. Please provide postal codes for all affiliations.
 - 5—Please verify that the mailing address and e-mail address for correspondence are correct as set.
 - 6—If your proof includes supplementary material, please confirm that all supplementary material is cited in the text.
 - 7—If your proof includes links to Web sites, please verify that the links are valid and will direct readers to the correct Web page.
 - 8—“APC” was spelled out as “allophycocyanin” per journal guidelines, because APC is the standard abbreviation for “Ag-presenting cell.” Please amend or confirm.
 - 9—Changed “RPMI” to “RPMI 1640.” Please amend or confirm (“Complete RPMI. . .”).
 - 10—Please spell out “NEAA” at its only use in the text, and delete the abbreviation (“Complete RPMI. . .”).
 - 11—Please confirm that this accession number is being reported on for the first time.
 - 12—Is “mean fluorescence intensity” the correct expansion for “MFI”? (“Interestingly, we. . .”).
 - 13—Please confirm that all potential conflicts of interest have been disclosed.
 - 14—Please clarify the use of “±” in the legend for Fig. 1A (“Lineage markers...”).
 - 15—Added the locant for panel D in the legend for Fig. 1. Please amend or confirm that it is in the correct location.
 - 16—If your proof includes figures, please check the figures in your proof carefully. If any changes are needed, please provide a revised figure file.
 - 17—Is “false-discovery rate” the correct expansion for “FDR” in the legend for Fig. 6?
-
-